

1 **AOD distributions and trends of major aerosol species over a selection of the world's most**  
2 **populated cities based on the 1st Version of NASA's MERRA Aerosol Reanalysis**

3 Simon Provençal<sup>1\*</sup>, Pavel Kishcha<sup>2</sup>, Arlindo M. da Silva<sup>3</sup>, Emily Elhacham<sup>2</sup> and Pinhas Alpert<sup>2</sup>

4 <sup>1</sup> Département de géographie, Université Laval, Quebec City, Quebec, Canada

5 <sup>2</sup> Department of Geosciences, Tel Aviv University, Tel Aviv, Israel

6 <sup>3</sup> Goddard Space Flight Center, National Aeronautics and Space Administration, Greenbelt,  
7 Maryland, USA

8 \* Corresponding author: simon.provencal.1@ulaval.ca  
9

10 **Abstract**

11 NASA recently extended the Modern-Era Retrospective Analysis for Research and  
12 Application (MERRA) with an atmospheric aerosol reanalysis which includes five particulate  
13 species: sulfate, organic matter, black carbon, mineral dust and sea salt. The MERRA Aerosol  
14 Reanalysis (MERRAero) is an innovative tool to study air quality issues around the world for its  
15 global and constant coverage and its distinction of aerosol speciation expressed in the form of  
16 aerosol optical depth (AOD). The purpose of this manuscript is to apply MERRAero to the study  
17 of urban air pollution at the global scale by analyzing the AOD over a period of 13 years (2003–  
18 2015) and over a selection of 200 of the world's most populated cities in order to assess the impacts  
19 of urbanization, industrialization, air quality regulations and regional transport which affect urban  
20 aerosol load. Environmental regulations and the recent global economic recession have helped to  
21 decrease the AOD and sulfate aerosols in most cities in North America, Europe and Japan. Rapid  
22 industrialization in China over the last two decades resulted in Chinese cities having the highest  
23 AOD values in the world. China has nevertheless recently implemented emission control measures  
24 which are showing early signs of success in many cities of Southern China where AOD has  
25 decreased substantially over the last 13 years. The AOD over South American cities, which is  
26 dominated by carbonaceous aerosols, has also decreased over the last decade due to an increase in  
27 commodity prices which slowed deforestation activities in the Amazon rainforest. At the opposite,  
28 recent urbanization and industrialization in India and Bangladesh resulted in a strong increase of  
29 AOD, sulfate and carbonaceous aerosols in most cities of these two countries. The AOD over most  
30 cities in Northern Africa and Western Asia changed little over the last decade. Emissions of natural  
31 aerosols, which cities in these two regions tend to be mostly composed of, don't tend to fluctuate  
32 significantly on an annual basis.  
33

34 **Keywords:** Urban air pollution; Aerosol optical depth (AOD); Sulfate; Particulate organic  
35 matter; Black carbon; Mineral dust; MERRAero.  
36

37 **1 Introduction**

38 Microscopic airborne aerosols have long been a prominent topic of study in the field of  
39 environmental science, predominantly in the atmospheric sciences. A considerable amount of  
40 literature has emerged in order to better understand the nature of these particles, but more  
41 specifically, to assess their impacts on various spheres of life and the environment. Aerosols are  
42 found in highly variable space and time distribution, size and chemical composition, and they

43 originate from many sources, both natural and anthropogenic (Pöschl, 2005).

44 Aerosols considerably affect the environment and its living organisms. It is well documented  
45 that aerosols are a serious health hazard to humans, fauna and flora. They are linked to  
46 cardiovascular, respiratory and allergic diseases, as well as enhanced mortality (Pöschl, 2005;  
47 Tager, 2013). Aerosols also affect weather and climate. Acting as cloud condensation nuclei,  
48 aerosols are an essential element of cloud formation. As such, they play an indirect role in  
49 increasing the clouds' and the Earth's albedo as a whole (Haywood and Boucher, 2000; Lohmann  
50 and Feichter, 2005). They also affect the Earth's radiation budget as absorbers of radiation,  
51 contributing to a warming of the atmosphere, and as reflectors of radiation, in which case they act  
52 as a cooling agent (Haywood and Boucher, 2000). Finally, in high enough concentration, they can  
53 significantly reduce visibility (Charlson, 1969; Cheng and Tsai, 2000). This is often associated  
54 with episodes of haze, smog and dust storms.

55 The seriousness of the impacts listed in the previous paragraph is dependent on the aerosol  
56 concentration and size, but particularly on its chemical composition. It is therefore relevant to  
57 distinguish between different aerosol species commonly found in the air:

- 58 • Sulfate (SO<sub>4</sub>) aerosols originate from sulfur dioxide (SO<sub>2</sub>) which has been neutralized by  
59 ammonium (NH<sub>4</sub>) to form ammonium sulfate ((SO<sub>4</sub>)<sub>2</sub>NH<sub>4</sub>, Forster *et al.*, 2007, sect. 2.4.4.1).  
60 SO<sub>2</sub> emissions emerge from fossil fuel and, to a much smaller extent, biomass burning, and  
61 therefore are vastly considered as anthropogenic. However, small natural contributions  
62 originate from volcanoes and the oceans (Haywood and Boucher, 2000);
- 63 • Nitrate (NO<sub>3</sub>) aerosols originate from nitrogen oxides (NO<sub>x</sub>) which has been neutralized by  
64 ammonium (NH<sub>4</sub>) to form ammonium nitrate (NO<sub>3</sub>NH<sub>4</sub>, Forster *et al.*, 2007, sect. 2.4.4.5).  
65 NO<sub>3</sub> emissions emanate from a variety of sources such as fossil fuel and biomass burning,  
66 which is why Delmas *et al.* (1997) estimated that 83% of NO<sub>3</sub> emissions are anthropogenic  
67 in nature. Natural sources of NO<sub>3</sub> include bacteria and lightning.
- 68 • Particulate organic matter (POM), made up largely of organic carbon (OC), is the result of  
69 fossil fuel and biomass burning. The former is an anthropogenic source while the latter can  
70 be either a natural or an anthropogenic source. As a whole, sources of POM are widely  
71 considered to be anthropogenic (Haywood and Boucher, 2000; Forster *et al.*, 2007, sect.  
72 2.4.4.3);
- 73 • Black carbon (BC) particles are the result of incomplete combustion and originate from the  
74 same sources as POM (Haywood and Boucher, 2000; Forster *et al.*, 2007, sect. 2.4.4.2);
- 75 • Mineral dust (DS) is the product of wind erosion predominantly in arid environments.  
76 Sources are therefore considered natural. However, deforestation, agricultural and industrial  
77 practices are responsible for a portion of anthropogenic dust aerosols in the atmosphere  
78 (Haywood and Boucher, 2000; Forster *et al.*, 2007, sect. 2.4.4.6; Denman *et al.*, 2007, sect.  
79 7.5.1.1).
- 80 • Sea salt (SS) aerosols originate from the oceans. The release of salt particles depends on  
81 meteorological factors such as surface wind speed and sea surface temperature (Denman *et*  
82 *al.*, 2007, sect. 7.5.1.2).

83 There is scientific interest in studying aerosol pollution in cities because associated industries  
84 and road traffic are major sources of particulate matter and gaseous contaminants capable of  
85 forming aerosols through various chemical reactions and physical processes. Cities do offer a wide  
86 variety of opportunities such as employment, education, health care, entertainment and other  
87 services which stimulate an ongoing and accelerating urbanization movement around the world

88 (Moore *et al.*, 2003). The United Nations (2014) estimated that 30% of the world's population lived  
89 in an urban area in 1950. This proportion grew to 47% in 2000 and is expected to reach 66% in  
90 2050 (United Nations, 2014). Particularly in developing countries, where the rate of urbanization  
91 is the greatest (Subbotina, 2004, chap. 10), cities are lacking the means to adjust fast enough to  
92 fulfill the demand of its rapidly growing population and economic development. In this respect,  
93 urbanization comes with its fair share of environmental consequences (Sharma and Joshi, 2016).  
94 The phenomenon known as *global dimming* which consists of a significant decrease in solar  
95 radiation flux around the world since the 1950's is actually spatially inconsistent and much more  
96 pronounced over densely populated urban areas (Alpert *et al.*, 2005; Alpert and Kishcha, 2008).  
97 Indeed, atmospheric aerosol concentrations are significantly higher in populated cities as opposed  
98 to rural or remote areas (Cheng and Tsai, 2000), and the cities' population growth in developing  
99 countries tends to correlate with an increase of aerosol concentration (Kishcha *et al.*, 2011). Rapid  
100 urbanization and development in India and China resulted in a sharp increase of air pollutant  
101 emissions during the last decade (Lu *et al.*, 2011) and frequently recurring episodes of air pollution  
102 and haziness. On the other hand, urbanization in developed countries, albeit at a slower rate, hasn't  
103 had such a negative impact. Developed countries did indeed struggle with severe air pollution  
104 issues in the past, but their economic and democratic situation provides them with the means to  
105 enforce clean air regulations and develop green technologies. As a result, air quality has  
106 significantly improved over the last decades in the United States (Hand *et al.*, 2013), Europe  
107 (Vestreng *et al.*, 2007; Tørseth *et al.*, 2012) and Japan (Wakamatsu *et al.*, 2013) even though their  
108 population and economy kept on growing.

109 Several years ago, NASA's Global Modeling and Assimilation Office (GMAO) introduced  
110 the Modern-Era Retrospective Analysis for Research and Application (MERRA, Rienecker *et al.*,  
111 2011), a reanalysis tool incorporating satellite and model data to reproduce spatially consistent  
112 observations for many environmental variables. While the original MERRA included only  
113 meteorological parameters (wind, temperature, humidity, etc.), it has recently been extended to  
114 include assimilation of biased-corrected aerosol optical depth (AOD) from the Moderate  
115 Resolution Imaging Spectroradiometers sensors (MODIS, Remer *et al.*, 2005) on board the Aqua  
116 and Terra satellites, which led to its rebranding now known as MERRAero. Although only total  
117 AOD is constrained by MODIS observations, the data assimilation algorithm in MERRAero  
118 provides speciated hourly data, with the relative contributions from five of the major aerosol  
119 species listed previously. Version 1 of MERRAero doesn't assimilate NO<sub>3</sub> particles. Nevertheless,  
120 MERRAero provides an innovative tool to the scientific community to study aerosol pollution  
121 issues around the world, especially in regions where reliable surface-based monitoring is scarce or  
122 unavailable. Examples of MERRAero's applicability can be found in Kessner *et al.* (2013), Colarco  
123 *et al.* (2014), Kishcha *et al.* (2014; 2015) and Yi *et al.* (2015).

124 In this study, AOD data from MERRAero is used to assess the state of air quality over a large  
125 selection of major metropolitan areas around the world (hereafter simply referred to as "cities")  
126 over the last thirteen years (2003–2015). Speciation data is used to determine which aerosol species  
127 contribute most to AOD over each city and a trend analysis is performed to evaluate how local and  
128 regional factors, as well as natural and anthropogenic factors, affect aerosol pollution in urban  
129 environments. Alpert *et al.* (2012) previously and similarly analyzed AOD trends over a selection  
130 of major cities around the world based on MODIS data. The advantage of using MERRAero as  
131 opposed to just MODIS data is its ability to distinguish between aerosol species which provides  
132 substantially more information for analysis.

133

## 134 2 Methodology and data

### 135 2.1 MERRA Aerosol Reanalysis

136 NASA's Version 1 of MERRAero incorporates the latest version of the Goddard Earth  
137 Observing System (GEOS-5). It contains components for atmospheric circulation and composition  
138 (including atmospheric data assimilation), ocean circulation and biogeochemistry, and land surface  
139 processes. GEOS-5 also includes an atmospheric particulate matter (PM) module (Colarco *et al.*,  
140 2010, and references therein). This module is based on a version of the Goddard Chemistry,  
141 Aerosol, Radiation and Transport (GOCART) model (Chin *et al.*, 2002). GOCART treats the  
142 sources, sinks and chemistry of SO<sub>4</sub>, OC, BC, DS and SS particles. DS and SS emissions are a  
143 function of surface properties and wind speed at the surface. Sources of other species are simulated  
144 from emission inventories, including their precursors. SO<sub>2</sub> anthropogenic emissions are input from  
145 the Emission Database for Global Atmospheric Research (EDGAR) version 4.1 inventory from  
146 2005 and biomass burning emissions (primarily OC and BC) are input from the NASA Quick Fire  
147 Emission Dataset (QFED) version 2.1 (Buchard *et al.*, 2015). PM species are treated as external  
148 mixtures and do not interact with each other. MERRAero also assimilates bias-corrected AOD  
149 observations from the MODIS sensor on both Terra and Aqua. MERRAero reproduces the  
150 concentrations of all five particulate species modeled by GOCART and their relative AOD  
151 contributions all over the world every hour with a resolution of 0.5° latitude by 0.625° longitude  
152 from mid-2002 to 2015.

153 A number of MERRAero components have been evaluated in different regions of the world.  
154 Its assimilation of AOD has been validated over Africa, South America, Central and Eastern Asia  
155 using many remote sensing instruments by Buchard *et al.* (2015); Nowotnick *et al.* (2015)  
156 evaluated its aerosol speciation and vertical structure specific to Saharan dust transport using the  
157 Cloud-Aerosol Lidar with Orthogonal Polarization (CALIOP); in the United States, the surface  
158 concentrations of SO<sub>2</sub>, fine PM and its chemical speciation has been thoroughly evaluated by  
159 Buchard *et al.* (2014; 2016); in Europe, an evaluation of the surface concentrations of PM, fine PM  
160 and some of their chemical speciation has been performed by Provençal *et al.* (2017a); and finally,  
161 the surface concentration of fine PM in Israel and Taiwan was carried out by Provençal *et al.*  
162 (2017b).

### 164 2.2 Method

165 A selection of 200 of the world's most populated cities was chosen, inspired by Brinkhoff's  
166 major agglomerations list (City Population, <http://www.citypopulation.de>). All the selected cities  
167 have a population of at least 2 million inhabitants. Over every one of them, hourly AOD data from  
168 MERRAero were extracted for a period of 13 years, from 2003 to 2015, for total and every one of  
169 the five aerosol species. It is worth mentioning that MERRAero's resolution is too coarse to capture  
170 the urban core of cities. Urban aerosol load is obviously considered in the simulation, but urban  
171 grid points are broadly representative of the metropolitan areas, including the urban core and the  
172 surrounding suburbs.

173 A first analysis is performed by averaging the data over the 13-year period over each city and  
174 regrouping the cities by geographical region to determine their aerosol signature. A second analysis  
175 is performed by averaging the data by year over each city, calculating a regression trend over the  
176 13 years and performing a Student's *t*-test to evaluate the trend's significance at the 90% confidence

177 level. This will quantify the consequences of rapid urbanization with respect to air quality as well  
178 as ascertain the effectiveness of air pollution control over the last decade. The results are presented  
179 in map form. All the numerical data used to produce these maps are included in the supplementary  
180 material.  
181

### 182 3 AOD distributions of aerosol speciation (2003–2015)

#### 183 3.1 North and Central America

184 The proportions of aerosol species to total AOD for a selection of major cities in North and  
185 Central America are shown in Fig. 1. The reader is referred to the supplementary material for the  
186 actual AOD values. Highest urban AOD values are observed in Central and Eastern United States  
187 and Canada, ranging from 0.133 in Miami to 0.190 in Houston. Denver is an exception with the  
188 lowest mean AOD in the whole region (0.095). The Northeastern United States is highly populated  
189 and industrialized, which explains the higher AOD values in Philadelphia (0.190), Cincinnati  
190 (0.189), Washington (0.188), New York City (0.187), Pittsburg (0.184), Cleveland (0.181) and St.  
191 Louis (0.180). SO<sub>4</sub> aerosols account for a majority (> 50%) of total AOD in most North American  
192 cities. This is in line with Hand *et al.* (2012) who mentioned that the Eastern U.S. states emit  
193 substantially more sulfur dioxide (SO<sub>2</sub>), a precursor of SO<sub>4</sub> aerosols, compared to the other states.  
194 Overall, anthropogenic aerosols (SO<sub>4</sub>, POM and BC) represent at least 85% of total AOD in all the  
195 Northeastern cities. Nevertheless, overall, the mean AOD is relatively low (< 0.2) in all these cities.  
196 This is the result of effective air quality regulation in the U.S. known as the Clean Air Act, first  
197 adopted in 1970 and significantly amended in 1990. The success of this regulation has been  
198 highlighted by many (e.g., Granier *et al.*, 2011; de Meij *et al.*, 2012; Hand *et al.*, 2013; Xing *et al.*,  
199 2013, de Gouw *et al.*, 2014) by documenting a substantial reduction of SO<sub>2</sub> emissions and/or  
200 concentration, among other air pollutants, across the U.S. during the last decades. SO<sub>2</sub> emissions  
201 and SO<sub>4</sub> concentrations are generally well correlated (Hand *et al.*, 2013; Xing *et al.*, 2013).

202 Mean AOD values in Orlando (0.157), Tampa (0.152) and Miami (0.133) are among the  
203 lowest in the Eastern U.S. with a significantly stronger contribution from SS aerosol to total AOD  
204 (from 16% in Tampa to 26% in Miami) given their proximity to the Atlantic Ocean and the Gulf  
205 of Mexico, however, Buchard *et al.* (2016) and Provençal *et al.* (2016) documented a substantial  
206 overestimation of SS concentrations by MERRAero in coastal areas, therefore these SS proportions  
207 are likely overestimated as well.

208 The mean AOD in west coast cities is lower, from 0.107 in San Diego to 0.124 in Seattle, but  
209 the proportions of POM, BC and DS aerosols are higher. These cities are substantially affected by  
210 carbon emissions from wildfires occurring periodically in California, as opposed to solely  
211 anthropogenic sources. Indeed, Spracklen *et al.* (2007), who modeled OC emissions from summer  
212 wildfires in the Western U.S. between 1980 and 2004, concluded that variability of OC  
213 concentration in the Western U.S. is largely due to the variability of wildfire emissions.  
214 Furthermore, AOD values from MERRAero averaged by month, shown in Fig. 2(a) for Los  
215 Angeles, also suggest this to be the case. Aside from an increase caused by DS in spring, POM are  
216 largely responsible for the fluctuation of total AOD, particularly during the wildfire season between  
217 July and October. By contrast, the fluctuation of SO<sub>4</sub> AOD is barely perceivable. For the sake of  
218 comparison, the same graph is shown for New York City (Fig. 2(b)). The wintertime rainy season  
219 is also responsible, to a lesser extent, for the seasonal fluctuation. The fluctuations of SO<sub>4</sub> and POM  
220 AOD are much more correlated which suggests that carbonaceous aerosols originate largely from

221 energy consumption in that city. The higher DS proportion in the Western U.S. and Canadian cities  
222 is caused by advection of dust originating from the nearby deserts in the Southwestern U.S. and  
223 Northwestern Mexico.

224 The mean AOD in Mexican cities is relatively low (below 0.140) but its speciation signature  
225 is similar to Northeastern U.S. cities, dominated by SO<sub>4</sub> and POM aerosols. The Mexican  
226 government also implemented successful management programs and incentives to improve urban  
227 air quality during the last decades (Molina and Molina, 2004; Parrish *et al.*, 2011). Finally, AOD  
228 in Caribbean cities is also low (0.140 or less) but are much less impacted by anthropogenic aerosols.  
229 DS and SS compose over 50% of total AOD in Santo Domingo and San Juan. Indeed, the Caribbean  
230 receives a large amount of DS originating from the Sahara (Prospero and Mayol-Bracero, 2013).  
231

### 232 3.2 South America

233 The AOD distribution of aerosol speciation for cities located in South America is shown in  
234 Fig. 3. The mean AOD for cities in this region is somewhat lower compared to most cities in North  
235 America. Lima and Asunción are the only cities whose mean AOD is above 0.160. The speciation  
236 distribution is however quite different. The mean AOD in Buenos Aires and in cities of Southern  
237 Brazil is dominated by SO<sub>4</sub> and POM aerosols in more or less similar proportions. POM accounts  
238 for over half of total AOD in Goiânia, Brasília and Asunción. Deforestation and biomass burning  
239 for agricultural purposes in the Amazon rainforest are responsible for such a substantial presence  
240 of carbonaceous aerosols in the air (Sena *et al.*, 2013). Indeed, van der Werf *et al.* (2010) estimated  
241 that 14.5% of global carbon emissions from wildfires between 1997 and 2009 originate from South  
242 America. A synoptic circulation study published by Freitas *et al.* (2005) suggested that smoke  
243 plumes from wildfires in the Amazon are generally blown to the south which explains why POM  
244 contributes much less to total AOD in cities on the Brazilian east coast.

245 Fig. 4 compares the monthly averaged AOD between a city strongly impacted from wildfire  
246 emissions (Brasilia) and another one west of the Andes that is much less influenced by such  
247 emissions (Santiago). Brasilia is clearly affected by biomass burning emissions as shown by a sharp  
248 increase of POM, SO<sub>4</sub> and BC AOD during the wildfire season in the fall. Santiago, on the other  
249 hand, is slightly impacted by POM in the fall but its AOD distribution is overall dominated by SO<sub>4</sub>  
250 aerosols throughout the year. The impact of the summertime rainy season on the aerosol load over  
251 the west coast of South America is also clearly illustrated in Fig. 4(b).  
252

### 253 3.3 Africa

254 Fig. 5 displays the distribution of AOD speciation for cities located in Africa. The standout  
255 feature of Africa is obviously the Sahara desert which covers most of the northern part of the  
256 continent. DS emissions from the desert contribute to high AOD values observed in cities in  
257 vicinity of the desert, such as Kano (0.472), Dakar (0.402) and Khartoum (0.389). DS contributes  
258 to over 70% of total AOD in these three cities. DS contribute to ~50% of mean AOD in all other  
259 cities in Northern Africa. It is important to mention that MERRAero doesn't assimilate AOD data  
260 over bright surfaces such as deserts. Therefore, over the source region, the data is constrained  
261 primarily by parameterized emissions determined by wind speed. However, the darker surface of  
262 cities might have been sufficient to provide assimilated data in and around them.

263 The region of tropical Africa, south of the Sahara, is characterized by the savannah and  
264 rainforest where human-induced wildfires for agricultural purposes is a recurring practice and is an  
265 important source of aerosols (Archibald *et al.*, 2009; Eck *et al.*, 2003). Forest preservation  
266 initiatives have been implemented in Africa but Mercier (2012) essentially called them a failure.  
267 Over 50% of the world's carbon emissions from biomass burning does indeed originate from Africa  
268 (van der Werf *et al.*, 2010). Therefore, POM and BC aerosols together contribute to over 73% of  
269 total AOD in Kinshasa, 68% in Luanda and 56% in Harare. The influence of biomass burning  
270 aerosols diminishes toward South Africa where urban mean AOD is relatively low, from 0.084 in  
271 Cape Town to 0.180 in Durban. The aerosol signature in South African cities resemble most that  
272 of North American cities.  
273

### 274 **3.4 Europe, including Russia and Turkey**

275 The AOD proportions for cities located in Europe are shown in Fig. 6. The situation in  
276 European cities is, in many respects, similar to that of North American cities: mean AOD is  
277 relatively low while SO<sub>4</sub> aerosols contribute to ~50% or more to it in most cities. Europe is indeed  
278 a heavily industrialized continent but effective air quality regulations have also been implemented  
279 in Europe which resulted in a consistent emission and concentration decrease of various air  
280 pollutants, notably PM and SO<sub>2</sub>, over the last decades (Vestreng *et al.*, 2007; Granier *et al.*, 2011;  
281 Colette *et al.*, 2011; de Meij *et al.*, 2012; Tøseth *et al.*, 2012). Europe is however significantly  
282 impacted by the advection of DS originating from the Sahara desert which represents over 10% of  
283 total AOD in all European cities in Fig. 6. Cities closer to the Mediterranean Sea are the most  
284 impacted, which is in line with Barkan *et al.* (2005), Querol *et al.* (2009) and Pey *et al.* (2013) who  
285 analyzed Saharan dust transport over the Mediterranean and into Europe. Indeed, DS contributes  
286 to over 30% of total AOD in Izmir, Athens, Ankara and Naples, and to higher AOD values observed  
287 in cities such as Istanbul (0.206). Monthly averaged AOD values in Naples are offered as an  
288 example in Fig. 7 to show how much DS affects the AOD, especially in the spring when DS  
289 contributes almost as much as SO<sub>4</sub> to the total.

290 The mean AOD in cities of the northern and western parts of Europe tends to be lower, for  
291 instance in Madrid (0.104), Stockholm (0.119), Birmingham (0.122) and Lisbon (0.126). Even in  
292 the megacities of London and Paris, the total AOD is found to be fairly low (0.128 and 0.138,  
293 respectively), due to relatively low levels of SO<sub>4</sub> and a substantial reduction of SO<sub>2</sub> concentrations  
294 in London and Paris since the 1990's, but also in other European cities (Henschel *et al.*, 2013; Bigi  
295 and Harrison, 2010).  
296

### 297 **3.5 Western and Central Asia**

298 This region includes a selection of cities west of China and Myanmar which are shown in  
299 Fig. 8. Cities close to the Mediterranean Sea enjoy a relatively low aerosol load compared to other  
300 cities in this region of the world, from an AOD of 0.163 in Damascus to 0.219 in Tel Aviv. The  
301 AOD tends to increase toward Pakistan where the mean AOD in all Pakistani cities is above 0.4,  
302 except in Rawalpindi where it lies at 0.370. All cities in Western Asia are characterized by the  
303 prominent presence of DS particles due to their location in the Middle Eastern deserts. DS accounts  
304 for over 40% of total AOD in all cities of Western Asia and close to 70% in Riyadh and Baghdad.  
305 The large presence of DS in Pakistani cities is compounded by the significant presence of SO<sub>4</sub>  
306 aerosols, which explains their large overall AOD. The mean AOD from SO<sub>4</sub> aerosols is indeed the

307 highest in the Pakistani cities. Even if SO<sub>4</sub> AOD is lower in the other cities of Western Asia, SO<sub>4</sub>  
308 aerosols still provide an important contribution to total AOD in Tehran (41%), Aleppo (38%) and  
309 Tashkent (36%).

310 India is the world's second most populated country. Fig. 8 includes 15 cities in India with a  
311 population over 2 million inhabitants. India is also the world's second largest emitter of  
312 anthropogenic aerosols. Its recent population and industrialization growth resulted in a constant  
313 increase of fuel consumption and emission of SO<sub>2</sub>, OC and BC since the 1990's (Lu *et al.*, 2011;  
314 Klimont *et al.*, 2013). This results in high AOD values in most Indian cities; mean AOD is above  
315 0.5 in Patna, Delhi, Kanpur and Lucknow. Indian cities are also affected very much so by the  
316 advection of DS from nearby sources, especially in the northern part of India. DS aerosols  
317 contribute to 40% of total AOD in Jaipur, 38% in Ahmedabad and in Delhi.

318

### 319 **3.6 Eastern Asia**

320 This region includes a selection of cities in China, Taiwan, Korea and Japan, which are shown  
321 in Fig. 9. China is the most populated country in the world and has recently been surging  
322 economically at the cost of deteriorating air quality. Indeed, Chinese cities record some of the  
323 highest speciated AOD averages in the world. Out of the 35 Chinese cities shown in Fig. 9, only  
324 three cities, Kunming, Ürümqi and Lanzhou, have a mean AOD value below 0.3. This highest mean  
325 AOD is observed in Chengdu (0.800), Wuhan (0.709) and Changsha (0.706). China is the world's  
326 largest anthropogenic aerosol emitter. Its energy consumption has increased drastically since 2000  
327 as well as its emissions of SO<sub>2</sub>, OC and BC (Lu *et al.*, 2011; Wang and Hao, 2012; Klimont *et al.*,  
328 2013). SO<sub>4</sub> aerosols account for the majority of mean AOD (> 50%) in all Chinese cities except  
329 for Ürümqi located in the northeast, far away from the densely populated eastern coast. The  
330 contribution of carbonaceous aerosols is also quite significant. Residential activities account for  
331 ~70% of OC and ~55% of BC emissions in China (Lu *et al.*, 2011). This results in a strong seasonal  
332 AOD fluctuation in many Chinese cities. The megacity of Guangzhou is presented as an example  
333 in Fig. 10 to highlight how fossil fuel and biomass burning, combined with frequent stagnating  
334 weather conditions, create very high levels of pollution in winter and early spring (Zhang and Cao,  
335 2015). Additionally, advection of DS from the Gobi desert in northern China and the Taklimakan  
336 desert in Western China, particularly in the spring (Sullivan *et al.*, 2007), is reflected in the higher  
337 DS proportions found in cities of Northern China.

338 Cities in Taiwan, Korea and Japan are not as polluted as Chinese cities, they are nonetheless  
339 influenced by emissions and advection of pollutants from China. Lu *et al.* (2010) estimated that a  
340 1% increase of SO<sub>2</sub> emissions in China leads to 1.15% and 0.71% increases in background SO<sub>2</sub>  
341 concentrations in South Korea and Japan respectively. The mean AOD is indeed fairly high in  
342 Pyongyang (0.436), Seoul (0.412) and Taipei (0.348). The fact that Japan is farther away from  
343 China is reflected in its cities' lower AOD values, ranging from 0.250 in Nagoya to 0.295 in  
344 Fukuoka. Air quality policies have also been in place since the 1960's in Japan. SO<sub>2</sub> emissions and  
345 concentrations decreased substantially since the 1970's (Kanada *et al.*, 2013; Wakamatsu *et al.*,  
346 2013).

347

### 348 **3.7 Southeastern Asia and Oceania**

349 Fig. 11 maps the AOD distribution for cities located in Southeastern Asia and Australia. The



350 highest mean AOD in this part of the world are found in Bangkok (0.280), Jakarta (0.266) and  
351 Yangon (0.235). Cities in Indonesia (Jakarta, Bandung and Surabaya) are mostly impacted by SO<sub>4</sub>  
352 aerosols (from 58% to 66% of total AOD). Yangon, Bangkok, Saigon, Kuala Lumpur and  
353 Singapore are affected by SO<sub>4</sub> and POM aerosols in more or less similar proportions. Deforestation  
354 in tropical Asia emits a substantial amount of carbonaceous particles in the air through biomass  
355 burning (Chang and Song, 2010). van der Werf *et al.* (2010) estimated that 9.5% of the world  
356 carbon emissions from wildfires originate from equatorial Asia. Manila and Cebu City in the  
357 Philippines are less impacted by POM and more affected by SS aerosols.

358 The mean AOD in the three Australian cities is fairly low: 0.093 in Melbourne, 0.095 in  
359 Brisbane and 0.113 in Sydney. Like other industrialized countries, Australia maintains air quality  
360 guidelines, below those in the U.S. and Europe, which are generally respected (Broome *et al.*,  
361 2015).  
362

## 363 4 AOD trends of aerosol speciation (2003–2015)

### 364 4.1 Total AOD

365 The linear trend between 2003 and 2015 for total AOD and for all the cities is mapped in Fig.  
366 12. The color grading is indicative of the level of change with lighter colors indicating an  
367 insignificant change. Globally, the AOD is decreasing in a wide majority of cities. The trends are  
368 negative in every single city of the Americas, except in Sacramento and Santiago where they are  
369 positive but insignificant. The decreases are significant in cities of Eastern Canada and U.S., and  
370 the southeastern part of South America. The strongest decreases are observed in Washington and  
371 Asunción. Cities where the trend is insignificant tend to be those least affected by SO<sub>4</sub> aerosols,  
372 notably on the western coast of Canada and the U.S., in the Caribbean and in Eastern Brazil.  
373 Similarly in Europe, the trends are significantly negative in every European city, except in  
374 Stockholm, Kiev, Moscow and St. Petersburg where they are negative but insignificant.

375 Trends in cities of Africa and Western Asia are generally insignificant, either positively or  
376 negatively. They are, however, significant and negatively strong (0.004 decrease per year) in the  
377 cities of Algiers, Accra, Abidjan, Ibadan, Lagos and Tunis. The situation in India and Bangladesh  
378 is quite different, where all cities exhibit a positive trend, many of which are significant and strong  
379 (0.004 increase per year).

380 The AOD is decreasing in most of the 38 cities of China and Taiwan, albeit at an insignificant  
381 rate. The trend is nonetheless significant in a few cities and strongly decreasing in three cities of  
382 Southern China (Guangzhou, Xiamen and Hong Kong). Guangzhou, one of China's most populated  
383 cities, is in fact the city where the AOD trend is the strongest in the world (decrease of 0.0072 per  
384 year). The trends are also strongly negative in all Japanese cities and in the North Korean capital  
385 of Pyongyang. In Southeastern Asia, the trends tend to be insignificant, with the exception of  
386 Manila and Cebu City in the Philippines and Bangkok in Thailand, who exhibit a significant  
387 decreasing AOD. Finally, the three cities in Australia display an insignificant AOD decrease.

388 A similar analysis is performed in the following subsections for the trends of AOD speciation  
389 which will provide explanations for the AOD trends observed in Fig. 12. The reader is referred to  
390 the supplementary material for the trend values in all the cities in for all species.  
391

## 392 4.2 AOD from SO<sub>4</sub> aerosols

393 SO<sub>4</sub> AOD trends are shown in Fig. 13. The trend is decreasing significantly in most cities of  
394 North America, especially in Eastern Canada and U.S., coinciding with the total AOD decrease  
395 observed in Fig. 11 and in line with the goals of the Clean Air Act referenced in Sect. 3.1. Over the  
396 last decade (2000–2010), SO<sub>4</sub> concentrations decreased in all regions of the U.S. but even more so  
397 over the Eastern U.S. (Hand *et al.*, 2012; 2013). Cities in Central and South America experienced  
398 insignificant changes in their SO<sub>4</sub> aerosol load, except in Santo Domingo where it significantly  
399 decreased and in Santiago where it significantly increased.

400 In European cities, SO<sub>4</sub> AOD trends are generally decreasing significantly in Western Europe  
401 and insignificantly in Eastern Europe. They are increasing in only two cities, Vienna and Ankara,  
402 albeit at insignificant rates. This again is the result of effective air quality regulations implemented  
403 in Europe where SO<sub>2</sub> emissions and, by extension, SO<sub>4</sub> concentrations have decreased over the last  
404 decade (2001–2010; de Meij *et al.*, 2012).

405 The decrease in North American and European cities was aided by the recent global economic  
406 recession. A few authors have dealt with the issue of economic slowdown and air quality, notably  
407 Vrekoussis *et al.* (2013) who documented a sharp decrease of various gaseous pollutants over  
408 Greece since 2008, Russell *et al.* (2012) who noticed a stronger-than-normal decrease of the NO<sub>2</sub>  
409 column over many U.S. cities during the recession and Castellanos and Boersma (2012) who  
410 arrived at the same conclusion for the whole of Europe. Our data suggest that SO<sub>4</sub> aerosols were  
411 impacted in a similar fashion, as shown in Fig. 14 for a selection of four megacities in the  
412 industrialized world. In New York City, the AOD of SO<sub>4</sub> aerosols started to decline in 2007 and  
413 took a sharp drop in 2010 before rebounding the following year; SO<sub>4</sub> AOD also suffered a sharp  
414 decline in 2010 in London; the AOD decreased in Moscow between 2007 and 2010; and the same  
415 variable has been steadily decreasing in Tokyo since 2006 but more steadily since 2008.

416 SO<sub>4</sub> AOD trends have changed insignificantly in most cities of Africa and Western Asia  
417 where SO<sub>4</sub> aerosols generally contribute little to total AOD. There are some exceptions, for  
418 instance, Tunis, Algiers, Abidjan, Accra, Lagos and Ibadan where SO<sub>4</sub> AOD trends are  
419 significantly decreasing, Kinshasa where it is strongly decreasing and Cairo where it is significantly  
420 increasing. Although the trends are weak in cities in the north of India and in Bangladesh, Indian  
421 cities are rather unique in the global landscape in the sense that India is the only country where  
422 cities experienced a strong increasing SO<sub>4</sub> AOD trend. Tianjin in China is the only other city in  
423 the world with such a trend. In fact, the trend is increasing in all but one city in India (Jaipur), albeit  
424 insignificantly in three cities, including the megacity of Delhi. This is the likely result of recent  
425 industrial development and population growth in India. Lu *et al.* (2011) estimated that SO<sub>2</sub>  
426 emissions increased by 35% between 2004 and 2010 in India.

427 The trend is insignificant in most Chinese cities, positively in the northern part and negatively  
428 in the central part. Cities in Southern China experienced a significant decrease, quite strong in some  
429 case (Guangzhou, Chengdu, Hong Kong and Nanning). Like India, China has also been  
430 experiencing rapid urbanization and industrialization over the last decade. A look at Fig. 13 in  
431 deceiving since only a small number of cities reveal an increasing trend, and an insignificant one  
432 in most of those cities for that matter. The reason for this is most likely due to emission patterns  
433 observed in China. Lu *et al.*'s (2011) estimates of Chinese SO<sub>2</sub> emissions showed little change  
434 between 2004 and 2010. However, this is the result of an 11% increase from 2004 to 2006 (peak  
435 year) and a slow decrease since then (9% decrease between 2006 and 2010). Other estimates vary

436 by numbers but all agree with peak emissions in 2006 and a slow decrease since then (Lu *et al.*,  
437 2010; Wang and Hao, 2012; Zhang *et al.*, 2012; Klimont *et al.*, 2013). Implementation of national  
438 comprehensive policies by the Chinese government in 2005 has been successful in this respect. The  
439 government also took advantage of international events such as the 2008 Beijing Olympics to  
440 temporarily and regionally push stricter air quality guidelines (Lin *et al.*, 2013). However, SO<sub>2</sub>  
441 emissions and their trends are very disproportionate throughout China (Zhao *et al.*, 2012a; Zhao *et al.*,  
442 2012b). Guangzhou and Beijing are offered as examples in Fig. 15. Guangzhou follows more  
443 closely the national trend: peak SO<sub>4</sub> AOD in 2006 and a slow decrease since then, although not  
444 continuous. The SO<sub>4</sub> AOD trend in Beijing is fairly stable throughout the period with slight  
445 fluctuations.

446 The significant and occasionally strong SO<sub>4</sub> AOD decrease in all of Japan's cities is due to  
447 Japan's air quality policies and to the recession, as mentioned previously, but also due to its position  
448 downwind from China. Since peak SO<sub>4</sub> AOD is observed in 2006 in Tokyo (Fig. 15(d)) and in  
449 other Japanese cities, coinciding with China's peak SO<sub>4</sub> emissions, it appears that Japan has also  
450 benefited from the air quality regulations implemented by the Chinese government. Trends are  
451 significantly decreasing in Yangon, Bangkok, Saigon and both Pilipino cities of Cebu City and  
452 Manila, while it is insignificant in Kuala Lumpur, Singapore, the three cities in Indonesia and the  
453 three cities in Australia.  
454

### 455 4.3 AOD from POM and BC aerosols

456 Since POM and BC particles originate from the same sources, their trend is similar across  
457 the cities (Figs. 16 and 17). Carbonaceous aerosols are also the by-product of fossil fuel burning,  
458 it is therefore intuitive to observe a decreasing AOD trend in cities where the SO<sub>4</sub> AOD is also  
459 decreasing, and vice versa. This is the case for cities in the Eastern U.S., European, Indian and  
460 Japanese cities. However, trends for carbonaceous particles and SO<sub>4</sub> don't always parallel since  
461 carbon also originate from natural sources such as wildfires, whose contribution can explain the  
462 discrepancy between the two. For instance, the variability and recurrence of wildfires in the  
463 Western U.S. are largely responsible for the variability of OC concentrations in the same region  
464 (Spracklen *et al.*, 2007). Sacramento in California is offered as an example in Fig. 18. POM AOD  
465 fluctuates frequently according to the intensity of wildfires, as opposed to SO<sub>4</sub> AOD which barely  
466 changes from one year to another. POM AOD has been steadily increasing since 2010, in  
467 conjunction with intensifying wildfire activities experienced in California in recent years. The trend  
468 was however deemed insignificant by the statistical test. A single episodic series of strong wildfires  
469 can also leave a profound impact on a city's aerosol signature. Western Russia was affected by an  
470 intense wildfire season during the summer of 2010 (Konovalov *et al.*, 2011), which explains the  
471 POM AOD peak in Moscow in 2010 (Fig. 14(c)). This peak is however probably underestimated  
472 since occasionally the smoke from the wildfires was so thick that MODIS incorrectly identified it  
473 as clouds (van Donkelaar *et al.*, 2011). Mean AOD from the Aerosol Robotic Network  
474 (AERONET) observations in Moscow during July and August 2010 were above 1 for many days  
475 and reached a daily average peak of 3.6 on August 7 (Huijnen *et al.* 2012). MERRAero's average  
476 of 1.5 for the same day pales in comparison. Without this wildfire episode, the POM AOD decrease  
477 in Moscow would have been significant.

478 As mentioned previously, wildfires in the Amazon rainforest are also an important source of  
479 carbonaceous aerosols in South America (Sena *et al.*, 2013). POM AOD is decreasing significantly  
480 in all both two South American cities, and quite strongly in three cities (Asunción, Porto Alegre

481 and Buenos Aires). In accordance, deforestation in the Amazon has sharply decreased since 2004  
482 which appears to have been the cause of conservation policies and economic factors (Malingreau  
483 *et al.*, 2012) which resulted in a decreased of carbon emissions (van der Werf *et al.*, 2010). Biomass  
484 burning also contributes a large amount of carbon aerosols in Equatorial Africa (Eck *et al.*, 2003);  
485 the POM and BC trends are however mostly insignificant in cities of that continent except in right  
486 below the Sahara where the trends have decreased significantly. Carbon emission estimates also  
487 suggest a decrease during the first half of our study period in Northern Hemisphere Africa (Lehsten  
488 *et al.*, 2009; van der Werf *et al.*, 2010).

489 The BC trend in five cities in Northern China (Zibo, Zhengzhou, Tianjin, Shijiazhuang and  
490 Beijing) has increased strongly, which doesn't coincide with the POM trend. In Southeastern and  
491 Australian cities, the AOD for carbonaceous particles is insignificant in all cities except in Manila  
492 and Sydney, where the trend has decreased significantly.  
493

## 494 **5 Discussion and conclusion**

495 The MERRA Aerosol Reanalysis was used to study urban air pollution issues around the  
496 world by using its assimilation of AOD observations and modeled concentrations of particulate  
497 matter over a 13-year period (2003–2015). MERRAero's differentiation of particle speciation  
498 makes it a unique and innovative tool capable of estimating the AOD of individual aerosol species  
499 with a global and constant coverage, unlike remote sensing instruments. This is particularly useful  
500 for studying urban air pollution since cities tend to exhibit a heterogeneous composition of aerosols.

501 The mean AOD was high ( $> 0.3$ ) in most cities of China, India, the Middle East, Northern  
502 and tropical Africa. At the opposite, it was relatively low ( $< 0.2$ ) in most cities of North America,  
503 South America, Europe, Australia and South Africa. The high AOD values observed in Northern  
504 African and Western Asian cities are caused mostly by their proximity to large and sandy deserts.  
505 Advection of dust also affects cities in India and Bangladesh but the high AOD averages in cities  
506 of these two countries is mostly the result of anthropogenic emissions of pollutants from fossil fuel  
507 burning activities. Fossil fuel burning is also responsible, for the most part, for the high AOD values  
508 observed in Chinese cities. However, advection of dust affects to some extent the AOD in cities of  
509 Northern China as well. High AOD averages in cities of tropical Africa are caused by deforestations  
510 and biomass burning activities.

511 Cities in North America, Europe, Japan, Southeastern Asia and Oceania tend to have a  
512 relatively low AOD on average, while  $\text{SO}_4$  and POM aerosols contribute to it most. Even though  
513 fossil fuel consumption is a major source of pollution in those parts of the world, effective air  
514 quality regulations have been successful at keeping emissions and, as a consequence, AOD values  
515 low over the last decade. Cities in South America and on the west coast of the U.S. are affected by  
516 fossil fuel burning but carbon emissions from wildfires contribute a significant proportion to their  
517 mean AOD during the summer. European cities are also affected by dust transport from the Sahara.

518 Overall,  $\text{SO}_4$  aerosols represent at least 10% of the mean AOD in all but two of the 200 cities  
519 presented in the various maps of this manuscript, those of Dakar in Senegal and Kano in Nigeria,  
520 for the only reason that their AOD is overwhelmed by DS particles due to their location close to  
521 the Sahara. POM aerosols represent at least 10% of the average in all but 24 cities, mostly located  
522 in Northern Africa or Western Asia. The presence of SS aerosols is significant in coastal cities but  
523 usually contributes little to the mean AOD.

524 The AOD decreased significantly between 2003 and 2015 in most cities of Eastern Canada  
525 and U.S., Europe and Japan, accompanied by an AOD decrease from SO<sub>4</sub>, POM and BC aerosols,  
526 a result of effective air quality regulations and the recent economic recession. Cities in South  
527 America, most of which have also experienced a significant AOD decrease, owe this decrease to a  
528 declining tendency of AOD from POM aerosols due to a slowdown of deforestation activities in  
529 the Amazon rainforest. At the opposite, all cities in India and Bangladesh experienced an increase  
530 of AOD from SO<sub>4</sub>, POM and BC aerosols which was quite strong in some cities due to recent and  
531 rapid urbanization and industrialization.

532 China has also been experiencing a strong urbanization and industrialization movement over  
533 the last decades which caused a strong increase in emissions of atmospheric pollutants. China has  
534 nevertheless implemented air quality guidelines during our study period which resulted in  
535 insignificant AOD trends in most Chinese cities. The regulations are however showing early signs  
536 of success with some cities in Southern China experiencing significant and strong decreases of  
537 AOD from SO<sub>4</sub> aerosols. The AOD values over Chinese cities are among the largest in the world,  
538 China therefore still has a lot of work to do before achieving the standard of other industrialized  
539 countries.

540 Many cities in Africa and all cities of Western Asia have seen little change in their aerosol  
541 load. Cities in this part of the world are mostly affected by aerosols originating from natural sources  
542 which don't tend to fluctuate significantly on timescales of a year or more. Maps for AOD trends  
543 from DS and SS aerosols were not shown or discussed for the simple reason that the trends were  
544 relatively weak and/or insignificant in most cities.

545 As demonstrated in this paper, MERRAero is an innovative tool that provides to the scientific  
546 community the means to study a broad range of aerosol pollution issues around the world. Some  
547 limitations pertaining to MERRAero are nevertheless worth raising. As mentioned previously, only  
548 MODIS AOD over oceans and dark land surfaces are assimilated. Furthermore, no vertically  
549 resolved aerosol information is available. NASA's Version 2 of MERRAero, MERRA-2,  
550 incorporates other remote sensing instruments, such as the Multi-angle Imaging Spectroradiometer  
551 (MISR) and the Aerosol Robotic Network (AERONET), into its reanalysis to mitigate this  
552 shortcoming. MERRA-2 is currently being analyzed and results will be reported in forthcoming  
553 publications.

554

## 555 **Acknowledgments**

556 This study was made with support from and in cooperation with the international Virtual  
557 Institute DESERVE (Dead Sea Research Venue) funded by the German Helmholtz Association.  
558

## 559 **References**

560 Alpert, P., Kishcha, P., Kaufman, Y.J., Schwarzbard, R., 2005. Global dimming or local dimming?:  
561 Effect of urbanization on sunlight availability. *Geophys. Res. Lett.* 32, L17802.

562 Alpert, P., Kishcha, P., 2008. Quantification of the effect of urbanization on solar dimming.  
563 *Geophys. Res. Lett.* 35, L08801.

564 Alpert, P., Shvainshtein, O., Kishcha, P., 2012. AOD trends over megacities based on space

- 565 monitoring using MODIS and MISR. *Am. J. Clim. Chang.* 1, 117–131.
- 566 Archibald, S., Roy, D.P., van Wilgen, B.W., Scholes, R.J., 2009. Why limits fire? An examination  
567 of drivers of burnt area in Southern Africa. *Glob. Chang. Biol.* 15, 613–630.
- 568 Barkan, J., Alpert, P., Kutiel, H., Kishcha, P., 2005. Synoptics of dust transportation days from  
569 Africa toward Italy and central Europe. *J. Geophys. Res.* 110, D07208.
- 570 Bigi, A., Harrison, R.M., 2010. Analysis of the air pollution climate at a central urban background  
571 site. *Atmos. Environ.* 44, 2004–2012.
- 572 Broome, R.A., Fann, N., Navin Cristina, T.J., Fulcher, C., Duc, H., Morgan, G.G., 2015. The health  
573 benefits of reducing air pollution in Sydney, Australia. *Environ. Res.* 143, 19–25.
- 574 Buchard, V., da Silva, A.M., Colarco, P., Krotkov, N., Dickerson, R.R., Stehr, J.W., Mount, G.,  
575 Spinei, E., Arkinson, H.L., He, H., 2014. Evaluation of GEOS-5 sulfur dioxide simulations during  
576 the Frostburg, MD 2010 field campaign. *Atmos. Chem. Phys.* 14, 1929–1941.
- 577 Buchard, V., da Silva, A.M., Colarco, P.R., Darmenov, A., Randles, C.A., Govindaraju, R., Torres,  
578 O., Campbell, J., Spurr, R., 2015. Using the OMI aerosol index and absorption aerosol optical depth  
579 to evaluate the NASA MERRA Aerosol Reanalysis. *Atmos. Chem. Phys.* 15, 5743–5760.
- 580 Buchard, V., da Silva, A.M., Randles, C.A., Colarco, P., Ferrare, R., Hair, J., Hostetler, C., Tackett,  
581 J., Winker, D., 2016. Evaluation of the surface PM<sub>2.5</sub> in Version 1 of the NASA MERRA Aerosol  
582 Reanalysis over the United States. *Atmos. Environ.* 125, 100–111.
- 583 Castellanos, P., Boersma, K.F., 2012. Reduction in nitrogen oxides over Europe driven by  
584 environmental policy and economic recession. *Sci. Rep.* 2, 265.
- 585 Charlson, R.J., 1969. Atmospheric visibility related to aerosol mass concentration. *Environ. Sci.*  
586 *Technol.* 3, 913–918.
- 587 Chang, D., Song, Y., 2010. Estimates of biomass burning emissions in tropical Asia based on  
588 satellite-derived data. *Atmos. Chem. Phys.* 10, 2335–2351.
- 589 Cheng, M.T., Tsai, Y.I., 2000. Characterization of visibility and atmospheric aerosols in urban,  
590 suburban, and remote areas. *Sci. Total Environ.* 263, 101–114.
- 591 Chin, M., Ginoux, P., Kinne, S., Torres, O., Holben, B., Duncan, B.N., Martin, R.V., Logan, J.,  
592 Higurashi, A., Nakajima, T., 2002. Tropospheric aerosol optical thickness from the GOCART  
593 model and comparisons with satellite and sun photometer measurements. *J. Atmos. Sci.* 59, 461–  
594 483.
- 595 Colarco, P., da Silva, A., Chin, M., Diehl, T., 2010. Online simulations of global aerosol  
596 distributions in the NASA GEOS-4 model and comparisons to satellite and ground-based aerosol  
597 optical depth. *J. Geophys. Res.* 115, D14207.
- 598 Colarco, P.R., Kahn, R.A., Remer, L.A., Levy, R.C., 2014. Impact of satellite viewing-swath width  
599 on global and regional aerosol optical thickness statistics and trends. *Atmos. Meas. Tech.* 7, 2313–  
600 2335.

- 601 Colette, A., Granier, C., Hodnebrog, Ø, Jakobs, H., Maurizi, A., Nyiri, A., Bessagnet, B.,  
602 d'Angiola, A., d'Isidoro, M., Gauss, M., Meleux, F., Memmesheimer, M., Mieville, A., Rouïl, L.,  
603 Russo, F., Solberg, S., Stordal, F., Tampieri, F., 2011. Air quality trends in Europe over the past  
604 decade: a first multi-model assessment. *Atmos. Chem. Phys.* 11, 11657–11678.
- 605 de Gouw, J.A., Parrish, D.D., Frost, G.J., Trainer, M., 2014. Reduced emissions of CO<sub>2</sub>, NO<sub>x</sub>, and  
606 SO<sub>2</sub> from U.S. power plants owing to switch from coal to natural gas with combined cycle  
607 technology. *Earth's Future* 2, 75–82.
- 608 de Meij, A., Pozzer, A., Lelieveld, J., 2012. Trend analysis in aerosol optical depths and pollutant  
609 emission estimates between 2000 and 2009. *Atmos. Environ.* 51, 75–85.
- 610 Delmas, R., Serça, D., Jambertm C., 1997. Global inventory of NO<sub>x</sub> sources. *Nutr. Cycl.*  
611 *Agroecosyst.* 48, 51–60.
- 612 Denman, K.L., Brasseur, G., Chidthaisong, A., Ciais, P., Cox, P.M., Dickinson, R.E., Hauglustaine,  
613 D., Heinze, C., Holland, E., Jacob, D., Lohmann, U., Ramachandran, S., da Silva Dias, P.L., Wofsy,  
614 S.C., Zhang, X., 2007. Couplings between changes in the climate system and biogeochemistry, in:  
615 Solomon, S., Qin, D., Manning, M., Chen, Z., Marquis, M., Averyt, K.B., Tignor, M. and Miller,  
616 H.L. (eds.), *Climate change 2007: the physical science basis*, Cambridge University Press,  
617 Cambridge, pp. 499–587.
- 618 Eck, T.F., Holben, B.N., Ward, D.E., Mukelabai, M.M., Dubovik, O., Smirnov, A., Schafer, J.S.,  
619 Hsu, N.C., Piketh, S.J., Queface, A., le Roux, J., Swap, R.J., Slutsker, I., 2003. Variability of  
620 biomass burning aerosol optical characteristics in Southern Africa during the SAFARI 2000 dry  
621 season campaign and a comparison of single scattering albedo estimates from radiometric  
622 measurements. *J. Geophys. Res.* 108, 8477.
- 623 Forster, P., Ramaswamy, V., Artaxo, P., Berntsen, T., Betts, R., Fahey, D.W., Haywood, J., Lean,  
624 J., Lowe, D.C., Myhre, G., Nganga, J., Prinn, R., Raga, G., Schulz, M., van Dorland, R., 2007.  
625 Changes in atmospheric constituents and in radiative forcing, in: Solomon, S., Qin, D., Manning,  
626 M., Chen, Z., Marquis, M., Averyt, K.B., Tignor, M., Miller, H.L. (eds.), *Climate change 2007: the*  
627 *physical science basis*, Cambridge University Press, Cambridge, pp. 129–234.
- 628 Freitas, S.R., Longo, K.M., Silva Dias, M.A.F., Silva Dias, P.L., Chatfield, R., Prins, E., Artaxo,  
629 P., Grell, G.A., Recuero, F.S., 2005. Monitoring the transport of biomass burning emissions in  
630 South America. *Environ. Fluid Mech.* 5, 135–167.
- 631 Granier, C., Bessagnet, B., Bond, T., d'Angiola, A., van der Gon, H.D., Frost, G.J., Heil, A., Kaiser,  
632 J.W., Kinne, S., Klimont, Z., Kloster, S., Lamarque, J.F., Liousse, C., Masui, T., Meleux, F.,  
633 Mieville, A., Ohara, T., Raut, J.C., Riahi, K., Schultz, M.G., Smith, S.J., Thompson, A., van  
634 Aardenne, J., van der Werf, G.R., van Vuuren, D.P., 2011. Evolution of anthropogenic and biomass  
635 burning emissions of air pollutants at global and regional scales during the 1980–2010 period.  
636 *Clim. Chang.* 109, 163–190.
- 637 Hand, J.L., Schichtel, B.A., Malm, W.C., Pitchford, M.L., 2012. Particulate sulfate ion  
638 concentration and SO<sub>2</sub> emission trends in the United States from the early 1990s through 2010.  
639 *Atmos. Chem. Phys.* 12, 10353–10365.
- 640 Hand, J.L., Schichtel, B.A., Malm, W.C., Pitchford, M., 2013. Widespread reductions in sulfate

- 641 across the United States since the early 1990s. *AIP Conf. Proc.* 1527, 495–498.
- 642 Haywood, J., Boucher, O., 2000. Estimates of the direct and indirect radiative forcing due to  
643 tropospheric aerosols: a review. *Rev. Geophys.* 38, 513–543.
- 644 Henschel, S., Querol, X., Atkinson, R., Pandolfi, M., Zeka, A., le Tertre, A., Analitis, A.,  
645 Katsouyanni, K., Chanel, O., Pascal, M., Bouland, C., Haluza, D., Medina, S., Goodman, P.G.,  
646 2013. Ambient air SO<sub>2</sub> patterns in 6 European cities. *Atmos. Environ.* 79, 236–247.
- 647 Huijnen, V., Flemming, J., Kaiser, J.W., Inness, A., Leitao, J., Heil, A., Eskes, H.J., Schultz, M.G.,  
648 Benedetti, A., Hadji-Lazarou, J., Dufour, G., Eremenko, M., 2012. Hindcast experiments of  
649 tropospheric composition during the summer 2010 fires over Western Russia. *Atmos. Chem. Phys.*  
650 12, 4341–4364.
- 651 Kanada, M., Fujita, T., Fujii, M., Ohnishi, S., 2013. The long-term impacts of air pollution control  
652 policy: historical links between municipal actions and industrial energy efficiency in Kawasaki  
653 City, Japan. *J. Clean. Prod.* 58, 92–101.
- 654 Kessner, A.L., Wang, J., Leby, R.C., Colarco, P.R., 2013. Remote sensing of surface visibility from  
655 space: a look at the United States east coast. *Atmos. Environ.* 81, 136–147.
- 656 Kishcha, P., Starobinets, B., Kalashnikova, O., Alpert, P., 2011. Aerosol optical thickness trends  
657 and population growth in the Indian subcontinent. *Int. J. Remote Sens.* 32, 9137–9149.
- 658 Kishcha, P., da Silva, A.M., Starobinets, B., Alpert, P., 2014. Air pollution over the Ganges basin  
659 and northwest Bay of Bengal in the early postmonsoon season based on NASA MERRAero data.  
660 *J. Geophys. Res.: Atmos.* 119, 1555–1570.
- 661 Kishcha, P., da Silva, A., Starobinets, B., Long, C., Kalashnikova, O., Alpert, P., 2015. Saharan  
662 dust as a causal factor of hemispheric asymmetry in aerosols and cloud cover over the tropical  
663 Atlantic Ocean. *Int. J. Remote Sens.* 36, 3423–3445.
- 664 Klimont, Z., Smith, S.J., Cofala, J., 2013. The last decade of global anthropogenic sulfur dioxide:  
665 2000–2011 emissions. *Environ. Res. Lett.* 8, 014003.
- 666 Konovalov, I.B., Beekmann, M., Kuznetsova, I.N., Yurova, A., Zvyagintsev, A.M., 2011.  
667 Atmospheric impacts of the 2010 Russian wildfires: integrating modelling and measurements of  
668 an extreme air pollution episode in the Moscow region. *Atmos. Chem. Phys.* 11, 10031–10056.
- 669 Lehsten, V., Tansey, K., Balzter, H., Thonicke, K., Spessa, A., Weber, U., Smith, B., Arneth, A.,  
670 2009. Estimating carbon emissions from African wildfires. *Biogeosciences* 6, 349–360.
- 671 Lin, J.T., Pan, D., Zhang, R.X., 2013. Trend and interannual variability of Chinese air pollution  
672 since 2000 in association with socioeconomic development: a brief overview. *Atmos. Ocean. Sci.*  
673 *Lett.* 6, 84–89.
- 674 Lohmann, U., Feichter, J., 2005. Global indirect aerosol effects: a review. *Atmos. Chem. Phys.* 5,  
675 715–737.
- 676 Lu, Z., Streets, D.G., Zhang, Q., Wang, S., Carmichael, G.R., Cheng, Y.F., Wei, C., Chin, M.,



- 677 Diehl, T., Tau, Q., 2010. Sulfur dioxide emissions in China and sulfur trends in East Asia since  
678 2000. *Atmos. Chem. Phys.* 10, 6311–6331.
- 679 Lu, Z., Zhang, Q., Streets, D.G., 2011. Sulfur dioxide and primary carbonaceous aerosol emissions  
680 in China and India, 1996–2010. *Atmos. Chem. Phys.* 11, 9839–9864.
- 681 Malingreau, J.P., Eva, H.D., de Miranda, E.E., 2012. Brazilian Amazon: a significant five year  
682 drop in deforestation rates but figures are on the rise again. *AMBIO* 41, 309–314.
- 683 Mercier, J.R., 2012. Revisiting deforestation in Africa (1990–2010): one more lost generation.  
684 *Madag. Conserv. Ecol.* 7, 5–8.
- 685 Molina, L.T., Molina, M.J., 2004. Improving air quality in megacities: Mexico City case study.  
686 *Ann. N.Y. Acad. Sci.* 1023, 142–158.
- 687 Moore, M., Gould, P., Keary, B.S., 2003. Global urbanization and impact on health. *Int. J. Hyg.*  
688 *Environ. Health* 206, 269–278.
- 689 Nowottnick, E.P., Colarco, P.R., Welton, E.J., da Silva, A., 2015. Use of the CALIOP vertical  
690 feature mask for evaluating global aerosol models. *Atmos. Meas. Tech.* 8, 3647–3669.
- 691 Parrish, D.D., Singh, H.B., Molina, L., Madronich, S., 2011. Air quality progress in North  
692 American megacities: a review. *Atmos. Environ.* 45, 7015–7025.
- 693 Pey, J., Querol, X., Alastuey, A., Forastiere, F., Stafoggia, M., 2013. African dust outbreaks over  
694 the Mediterranean basin during 2001–2011: PM<sub>10</sub> concentrations, phenomenology and trends, and  
695 its relation with synoptic and mesoscale meteorology. *Atmos. Chem. Phys.* 13, 1395–1410.
- 696 Pöschl, U., 2005. Atmospheric aerosols: composition, transformation, climate and health effects.  
697 *Angew. Chem. Int. Edit.* 44, 7520–7540.
- 698 Prospero, J.M., Mayol-Bracero, O.L., 2013. Understanding the transport and impact of African  
699 dust on the Caribbean basin. *Bull. Am. Meteorol. Soc.* 94, 1329–1337.
- 700 Provençal, S., Buchard, V., da Silva, A.M., Leduc, R., Barrette, N., 2017a. Evaluation of PM  
701 surface concentration simulated by Version 1 of the NASA MERRA Aerosol Reanalysis over  
702 Europe. *Atmos. Pollut. Res.* 8, 374–382.
- 703 Provençal, S., Buchard, V., da Silva, A.M., Leduc, R., Barrette, N., Elhacham, E., Wang, S.H.,  
704 2017b. Evaluation of PM<sub>2.5</sub> surface concentrations simulated by Version 1 of NASA's MERRA  
705 Aerosol Reanalysis over Israel and Taiwan. *Aerosol Air Qual. Res.* 17, 253–261.
- 706 Querol, X., Pey, J., Pandolfi, M., Alastuey, A., Cusack, M., Pérez, N., Monero, T., Viana, M.,  
707 Mihalopoulos, N., Kallos, G., Kleanthous, S., 2009. African dust contributions to mean ambient  
708 PM<sub>10</sub> mass-level across the Mediterranean basin. *Atmos. Environ.* 43, 4266–4277.
- 709 Remer, L.A., Kaufman, Y.J., Tanré, D., Mattoo, S., Chu, D.A., Martins, J.V., Li, R.R., Ichoku, C.,  
710 Levy, R.C., Kleidman, R.G., Eck, T.F., Vermote E., Holben, B.N., 2005. The MODIS aerosol  
711 algorithm, products, and validation. *J. Atmos. Sci.* 62, 947–973.

- 712 Rienecker, M.M., Suarez, M.J., Gelaro, R., Todling, R., Bacmeister, J., Liu, E., Bosilovich, M.G.,  
713 Schubert, S.D., Takacs, L., Kim, G.K., Bloom, S., Chen, J., Collins, D., Conaty, A., da Silva, A.,  
714 Gu, W., Joiner, J., Koster, R.D., Lucchesi, R., Molod, A., Owens, T., Pawson, S., Pegion, P.,  
715 Redder, C.R., Reichle, R., Robertson, F.R., Ruddick, A.G., Sienkiewicz, M., Woollen, J., 2011.  
716 MERRA: NASA's Modern-Era Retrospective Analysis for Research and Application. *J. Clim.* 24,  
717 3624–3648.
- 718 Russell, A.R., Valin, L.C., Cohen, R.C., 2012. Trends in OMI NO<sub>2</sub> observations over the United  
719 States: effects of emission control technology and the economic recession. *Atmos. Chem. Phys.*  
720 12, 12197–12209.
- 721 Sena, E.T., Artaxo, P., A.L. Correia, A.L., 2013. Spatial variability of the direct radiative forcing  
722 of biomass burning aerosols and the effects of land use change in Amazonia. *Atmos. Chem. Phys.*  
723 13, 1261–1275.
- 724 Sharma, R., Joshi, P.K., 2016. Mapping environmental impacts of rapid urbanization in the national  
725 capital region of India using remote sensing inputs. *Urban Clim.* 15, 70–82.
- 726 Spracklen, D.V., Logan, J.A., Mickley, L.J., Park, R.J., Yevich, R., Westerling, A.L., Jaffe, D.A.,  
727 2007. Wildfires drive interannual variability of organic carbon aerosol in the western U.S. in  
728 summer. *Geophys. Res. Lett.* 34, L16816.
- 729 Subbotina, T.P., 2004. Beyond economic growth: an introduction to sustainable development, 2nd  
730 ed. The International Bank for Reconstruction and Development, Washington.
- 731 Sullivan, R.C., Guazzotti, S.A., Sodeman, D.A., Prather, K.A., 2007. Direct observations of the  
732 atmospheric processing of Asian mineral dust. *Atmos. Chem. Phys.* 7, 1213–1236.
- 733 Tager, I.B., 2013. Health effects of aerosols: mechanisms and epidemiology, in: Ruzer, L.S.,  
734 Harley, N.H. (eds.), *Aerosols handbook: measurement, dosimetry, and health effects*, 2nd ed. CRC  
735 Press, Boca Raton, pp. 565–636.
- 736 Tørseth, K., Aas, W., Breivik, K., Fjæraa, A.M., Fiebig, M., Hjellbrekke, A.G., Lund Myhre, C.,  
737 Solberg, S., Yttri, K.E., 2012. Introduction to the European Monitoring and Evaluation Programme  
738 (EMEP) and observed atmospheric composition change during 1972–2009. *Atmos. Chem. Phys.*  
739 12, 5447–5481.
- 740 United Nations, 2014. World urbanization prospects, the 2014 revision.  
741 <http://esa.un.org/unpd/wup/CD-ROM/>. Accessed 1 December 2015.
- 742 van Donkelaar, A., Martin, R.V., Levy, R.C., da Silva, A.M., Krzyzanowski, M., Chubarova, N.E.,  
743 Semutnikova, E., Cohen, A.J., 2011. Satellite-based estimates of ground-level fine particulate  
744 matter during extreme events: a case study of the Moscow fires in 2010. *Atmos. Environ.* 45, 6225–  
745 6232.
- 746 van der Werf, G.R., Randerson, J.T., Giglio, L., Collatz, G.J., Mu, M., Kasibhatla, P.S., Morton,  
747 D.C., Defries, R.S., Jin, Y., van Leeuwen, T.T., 2010. Global fire emissions and the contribution  
748 of deforestation, savanna, forest, agricultural, and peat fires (1997–2009). *Atmos. Chem. Phys.* 10,  
749 11707–11735.

- 750 Vestreng, V., Myhre, G., Fagerli, H., Reis, S., Tarrason, L., 2007. Twenty-five years of continuous  
751 sulfur dioxide emission reduction in Europe. *Atmos. Chem. Phys.* 7, 3663–3681.
- 752 Vrekoussis, M., Richter, A., Hilboll, A., Burrows, J.P., Gerasopoulos, E., Lelieveld, J., Barrie, L.,  
753 Zarefos, C., Mihalopoulos, N., 2013. Economic crisis detected from space: air quality observations  
754 over Athens/Greece. *Geophys. Res. Lett.* 40, 458–463.
- 755 Wakamatsu, S., Morikawa, T., Ito, A., 2013. Air pollution trends in Japan between 1970 and 2012  
756 and impact of urban air pollution countermeasures. *Asian J. Atmos. Environ.* 7, 177–190.
- 757 Wang, S., Hao, J., 2012. Air quality management in China: issues, challenges, and options. *J.*  
758 *Environ. Sci.* 21, 2–13.
- 759 Xing, J., Pleim, J., Mathur, R., Pouliot, G., Hogrefe, C., Gan, C.M., Wei, C., 2013. Historical  
760 gaseous and primary aerosol emissions in the United States from 1990–2010. *Atmos. Chem. Phys.*  
761 13, 7531–7549.
- 762 Yi, B., Yang, P., Dessler, A., da Silva, A.M., 2015. Response of aerosol direct radiative effect to  
763 the East Asian summer monsoon. *IEEE Geosci. Remote Sens. Lett.* 12, 597–600.
- 764 Zhang, Q., He, K., Huo, H., 2012. Cleaning China’s air. *Nature* 484, 161–162.
- 765 Zhang, Y.L., Cao, F., 2015. Fine particulate matter (PM<sub>2.5</sub>) in China at a city level. *Sci. Rep.* 5,  
766 14884.
- 767 Zhao, B., Wang, S., Dong, X., Wang, J., Duan, L., Fu, X., Hao, J., Fu, J., 2013a. Environmental  
768 effects of the recent emission changes in China: implications for particulate matter pollution and  
769 soil acidification. *Environ. Res. Lett.* 8, 024031.
- 770 Zhao, Y., Zhang, J., Nielsen, C.P., 2013b. The effects of recent control policies on trends in  
771 emissions of anthropogenic atmospheric pollutants and CO<sub>2</sub> in China. *Atmos. Chem. Phys.* 13,  
772 487–508.
- 773

774 **Figure Captions**

775 **Fig. 1.** Proportion of aerosol speciation for a selection of cities in North and Central America.  
776 Mean AOD is provided for a few cities. The reader is referred to the supplementary  
777 material for such information for all the cities.

778 **Fig. 2.** AOD of total and aerosol species averaged by month in (a) Los Angeles and (b) New York  
779 City.

780 **Fig. 3.** Proportion of aerosol speciation for a selection of cities in South America.

781 **Fig. 4.** AOD of total and aerosol species averaged by month in (a) Brasilia and (b) Santiago.

782 **Fig. 5.** Proportion of aerosol speciation for a selection of cities in Africa.

783 **Fig. 6.** Proportion of aerosol speciation for a selection of cities in Europe.

784 **Fig. 7.** AOD of total and aerosol species averaged by month in Naples.

785 **Fig. 8.** Proportion of aerosol speciation for a selection of cities in Western and Central Asia.

786 **Fig. 9.** Proportion of aerosol speciation for a selection of cities in Eastern Asia.

787 **Fig. 10.** AOD of total and aerosol species averaged by month in Guangzhou.

788 **Fig. 11.** Proportion of aerosol speciation for a selection of cities in Southeastern Asia and Oceania.

789 **Fig. 12.** Linear trend for total AOD in all cities between 2003 and 2015.

790 **Fig. 13.** Linear trend for AOD from SO<sub>4</sub> aerosols in all cities between 2003 and 2015.

791 **Fig. 14.** AOD of total and aerosol species averaged by year in (a) New York City, (b) London, (c)  
792 Moscow and (d) Tokyo.

793 **Fig. 15.** AOD of total and aerosol species averaged by year in (a) Guangzhou and (b) Beijing.

794 **Fig. 16.** Linear trend for AOD from POM aerosols in all cities between 2003 and 2015.

795 **Fig. 17.** Linear trend for AOD from BC aerosols in all cities between 2003 and 2015.

796 **Fig. 18.** AOD of total and aerosol species averaged by year in Sacramento.

797

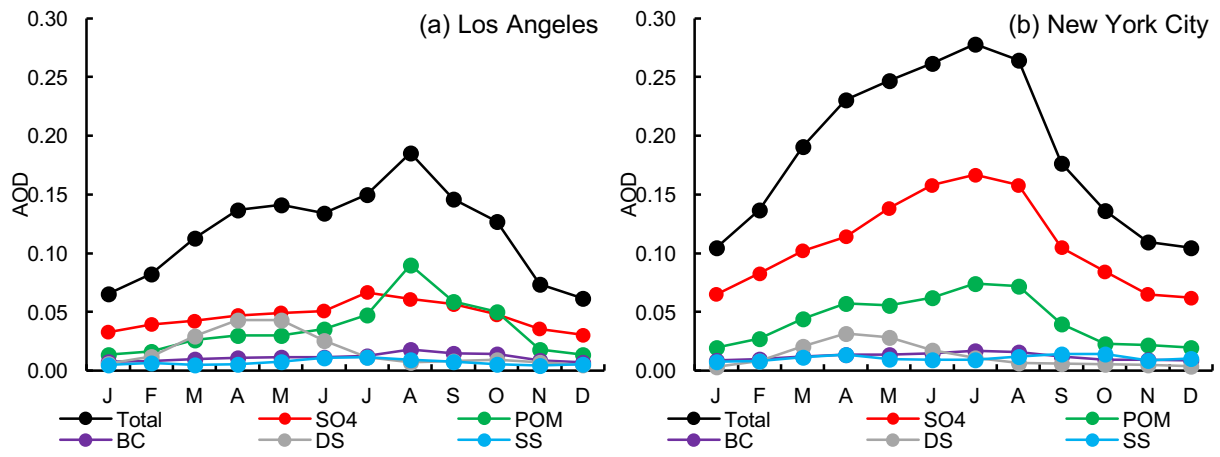


Fig. 2

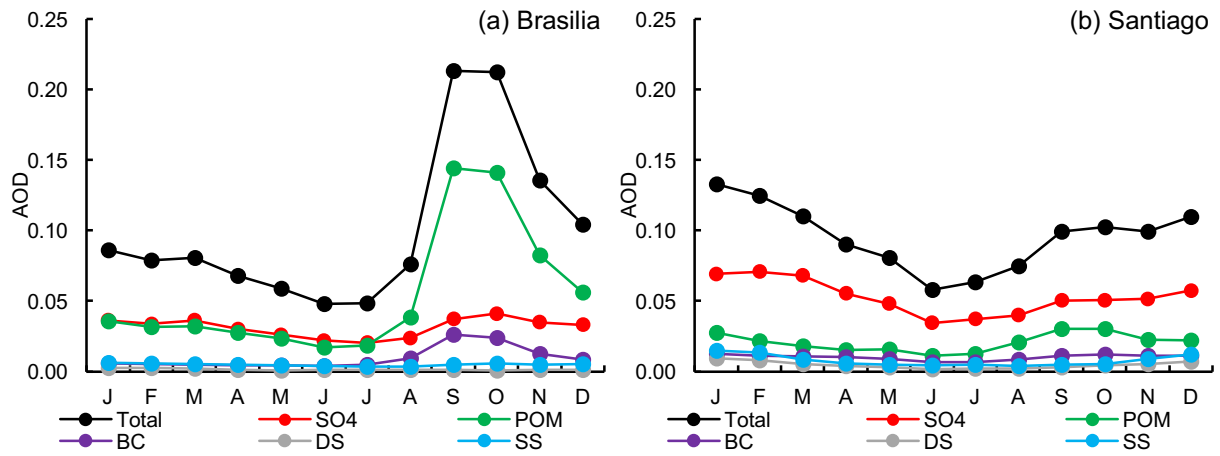


Fig. 4

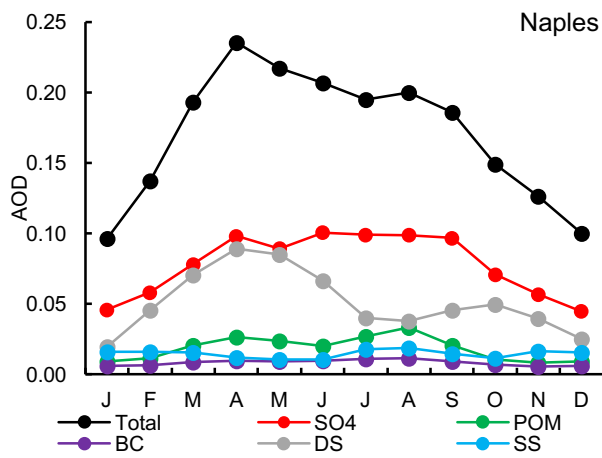


Fig. 7

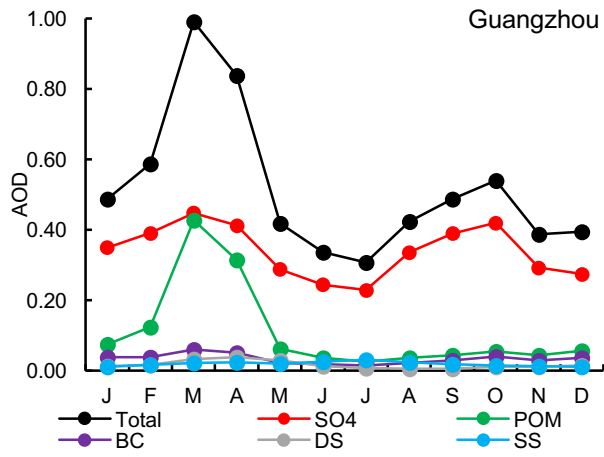


Fig. 10

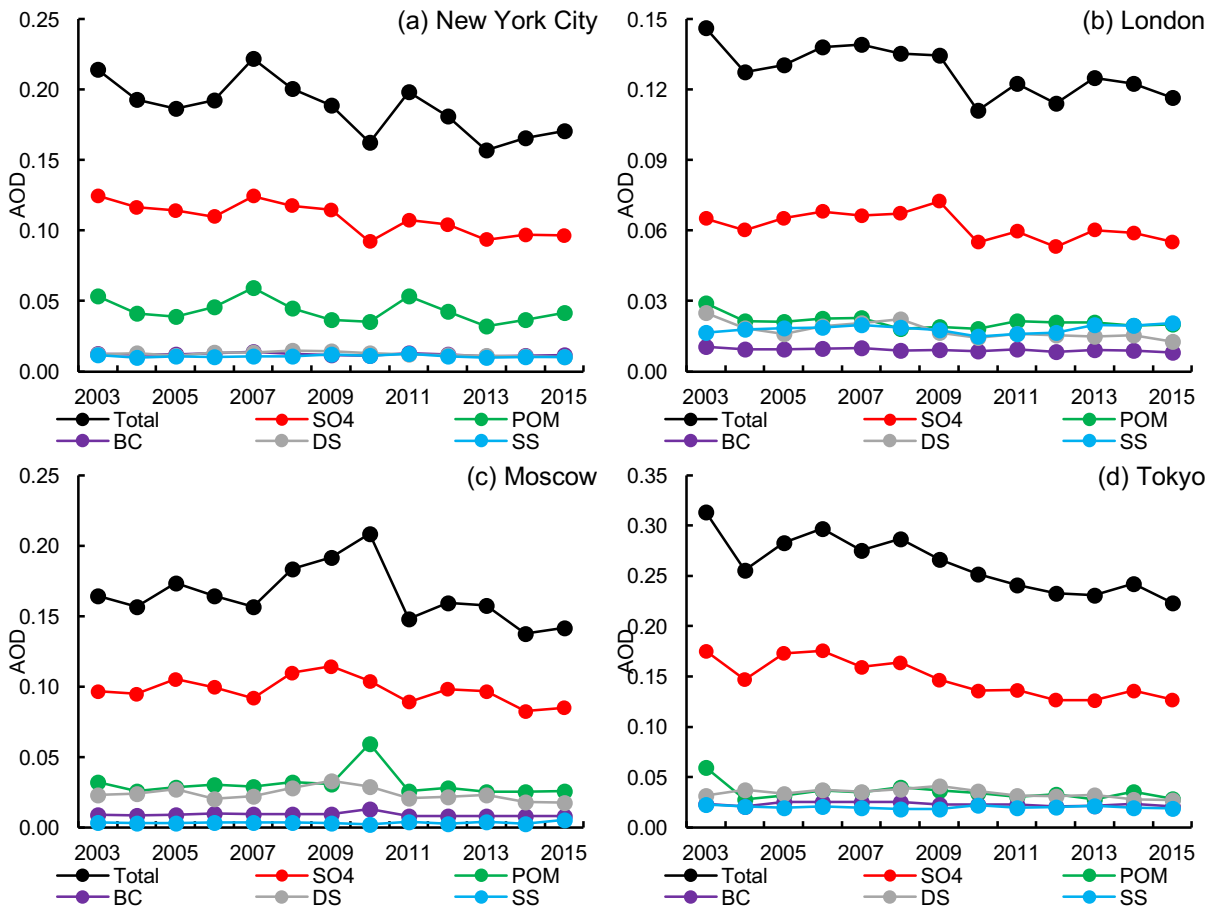


Fig. 14

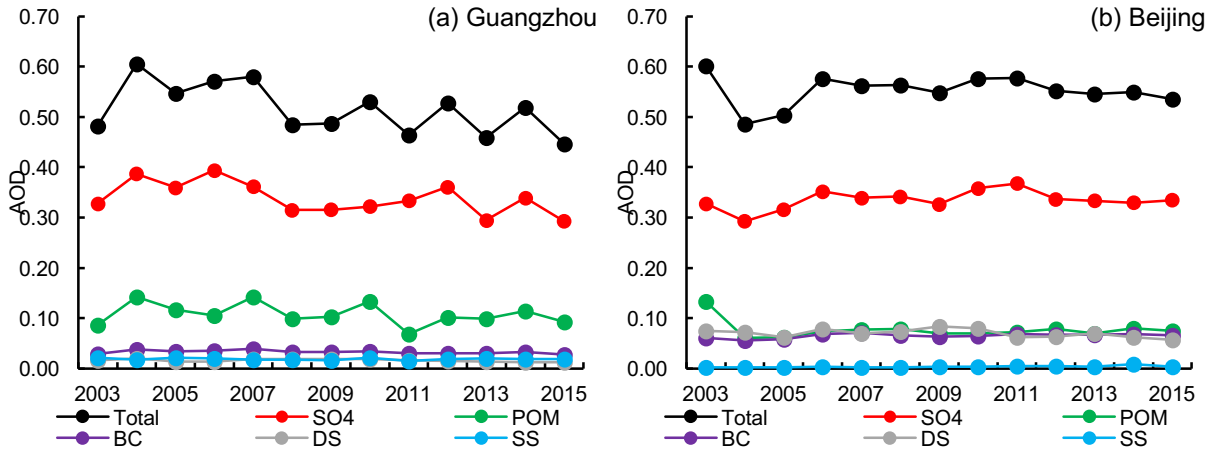


Fig. 15

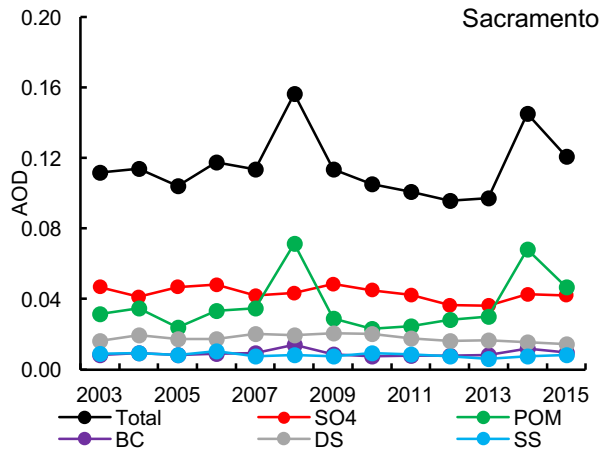


Fig. 18

Figure 1

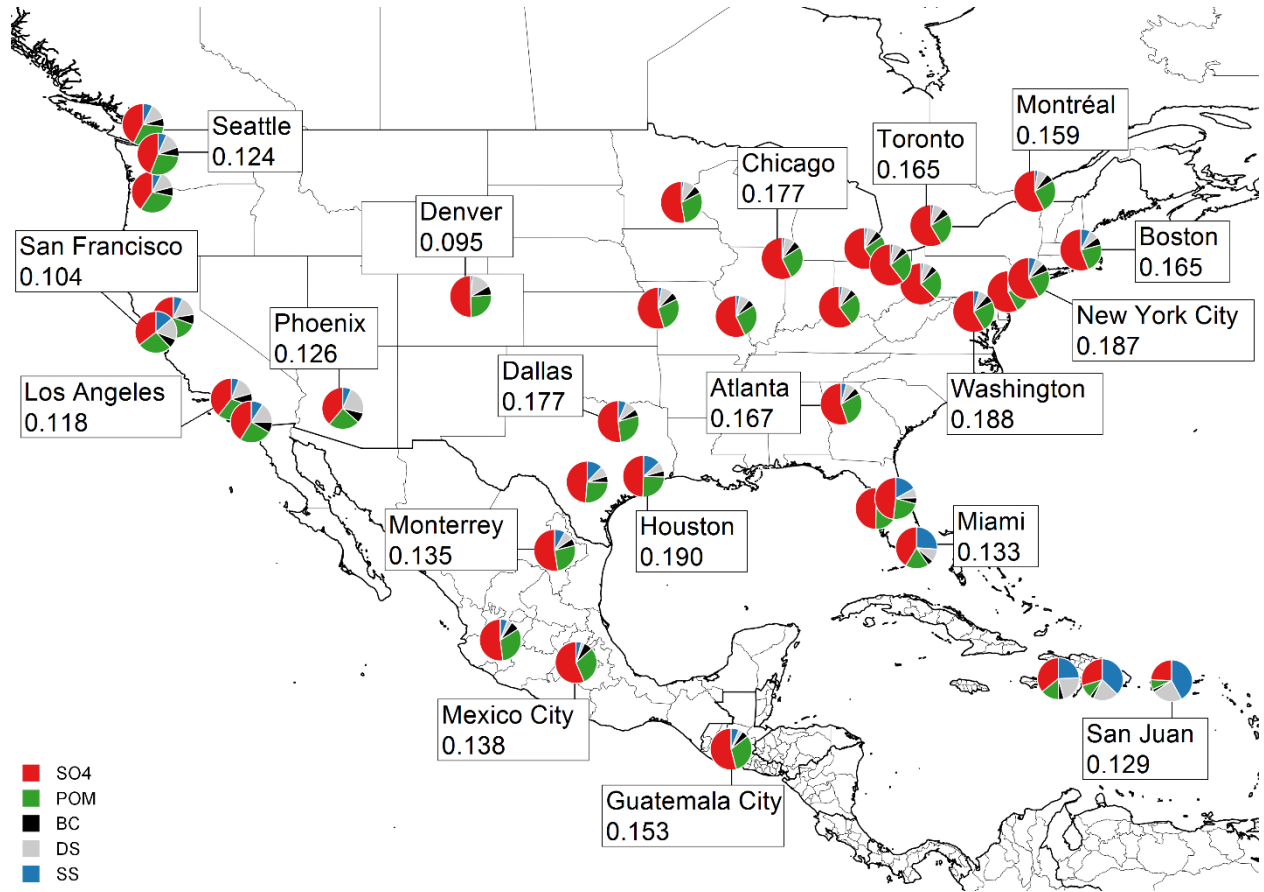




Figure 3

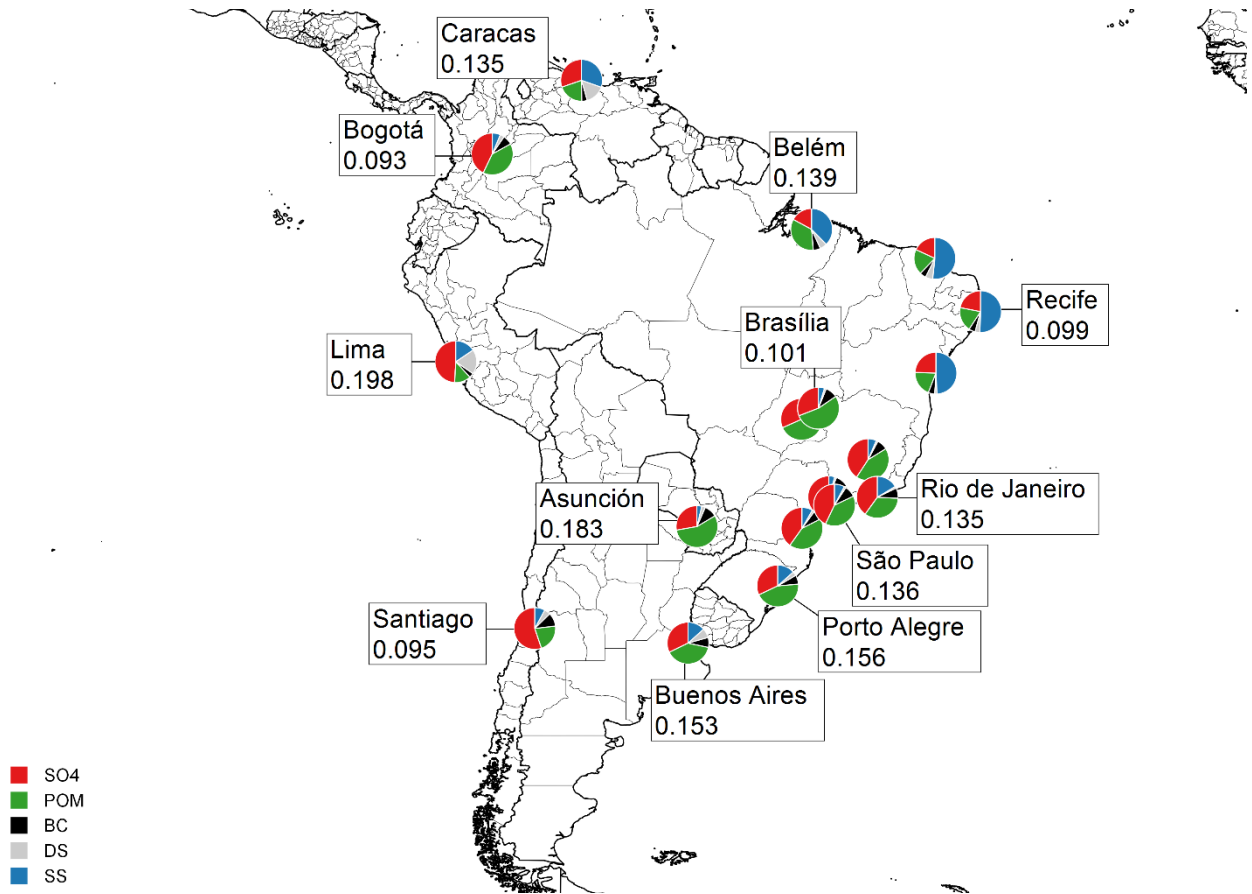


Figure 5

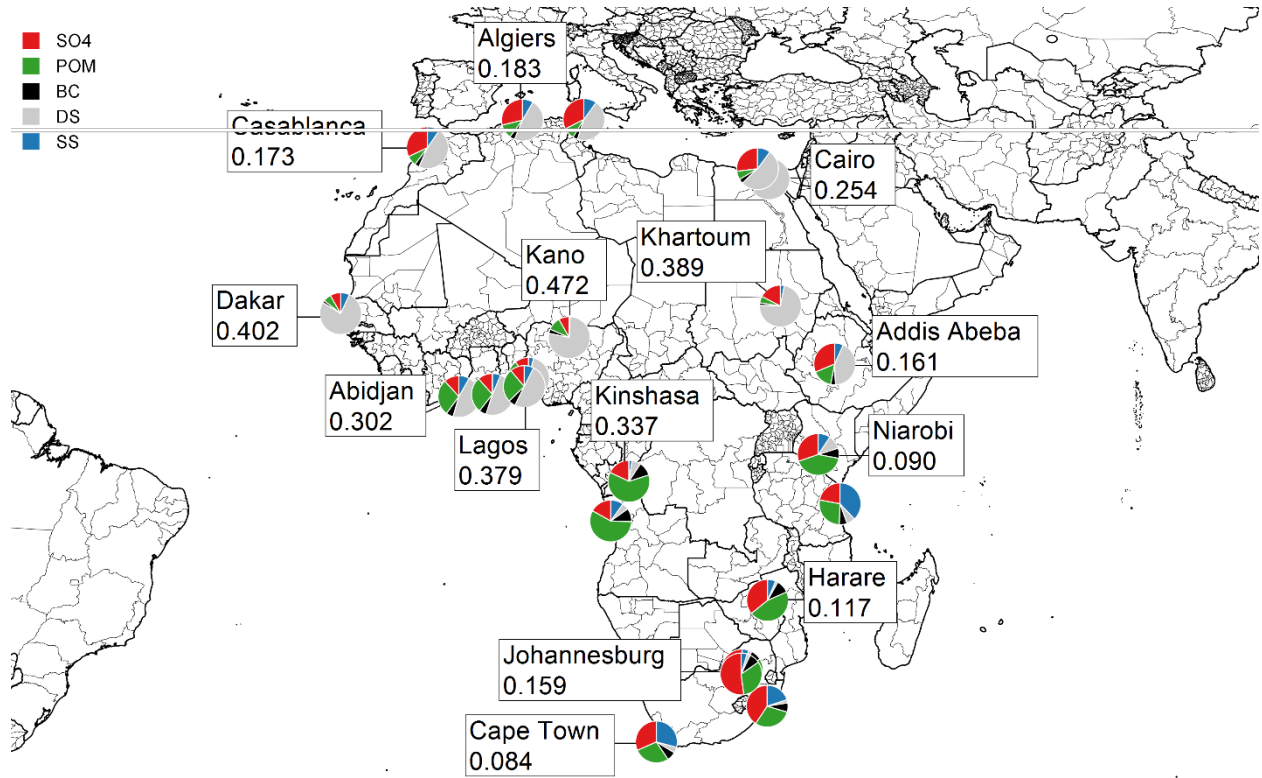


Figure 6

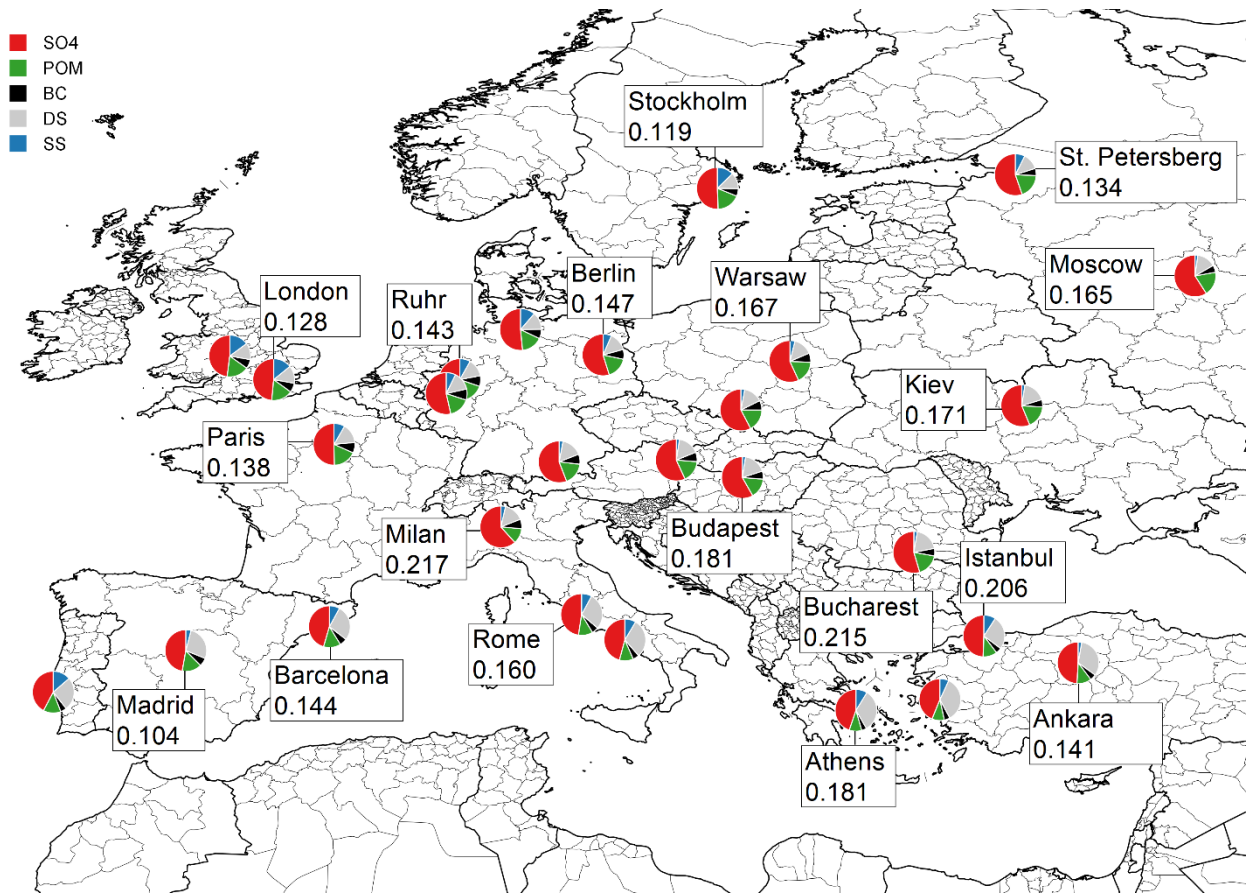


Figure 8

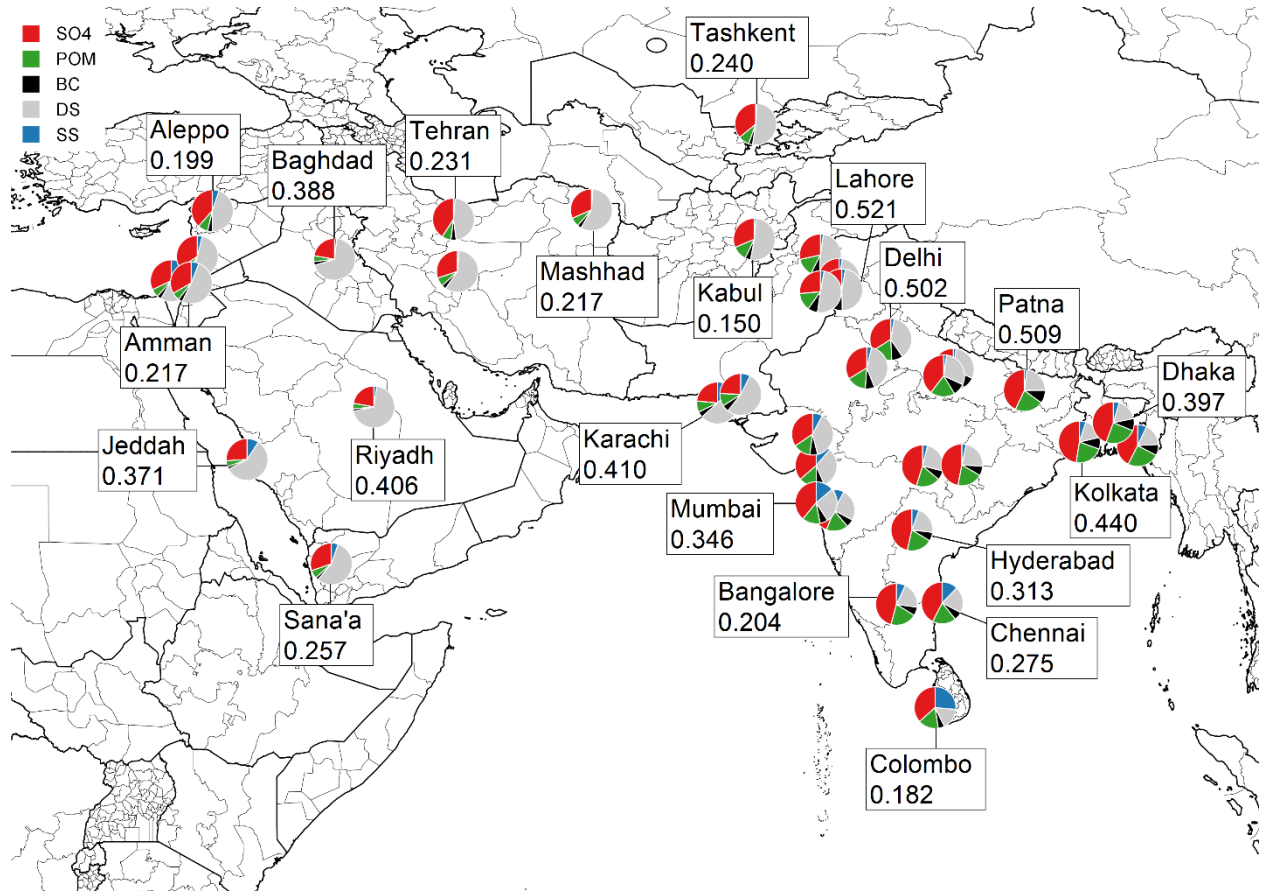


Figure 9

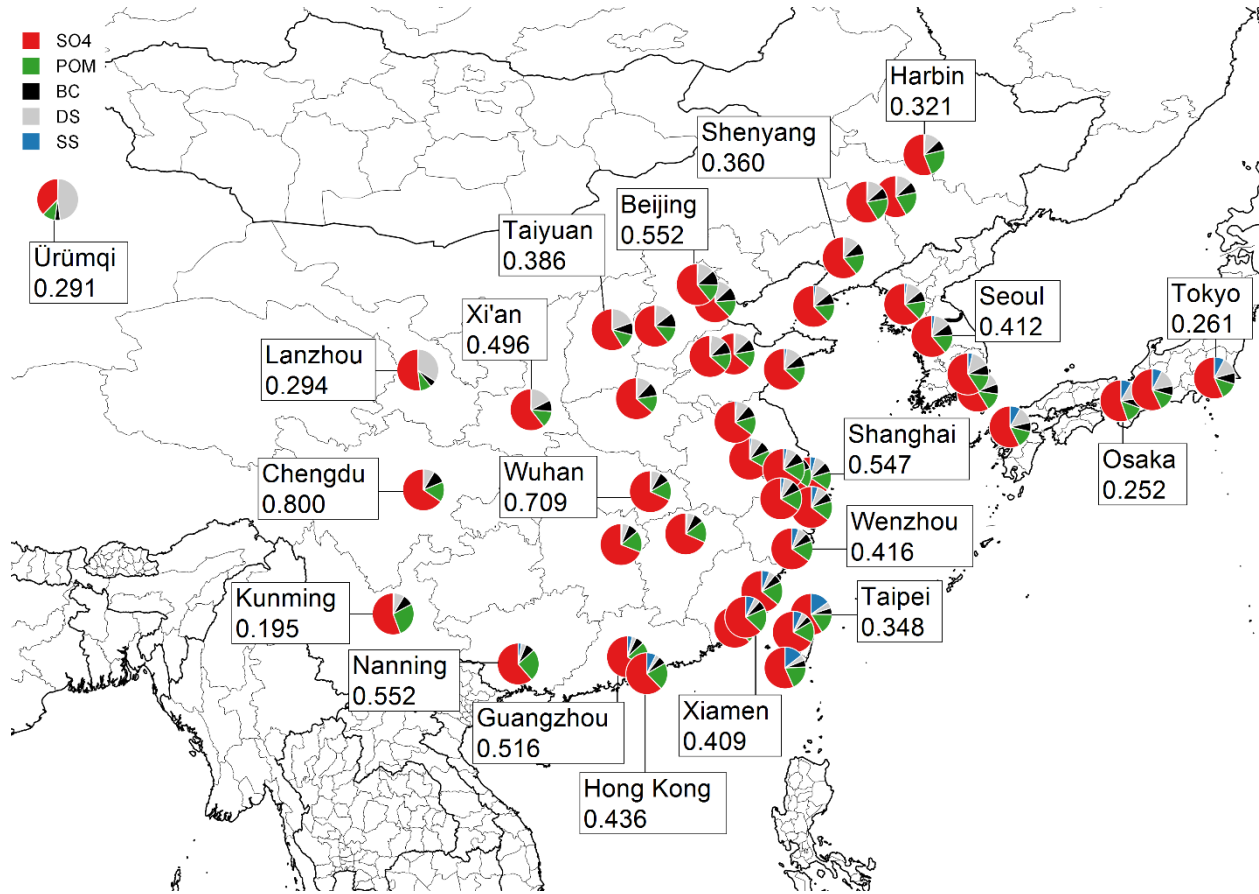


Figure 11

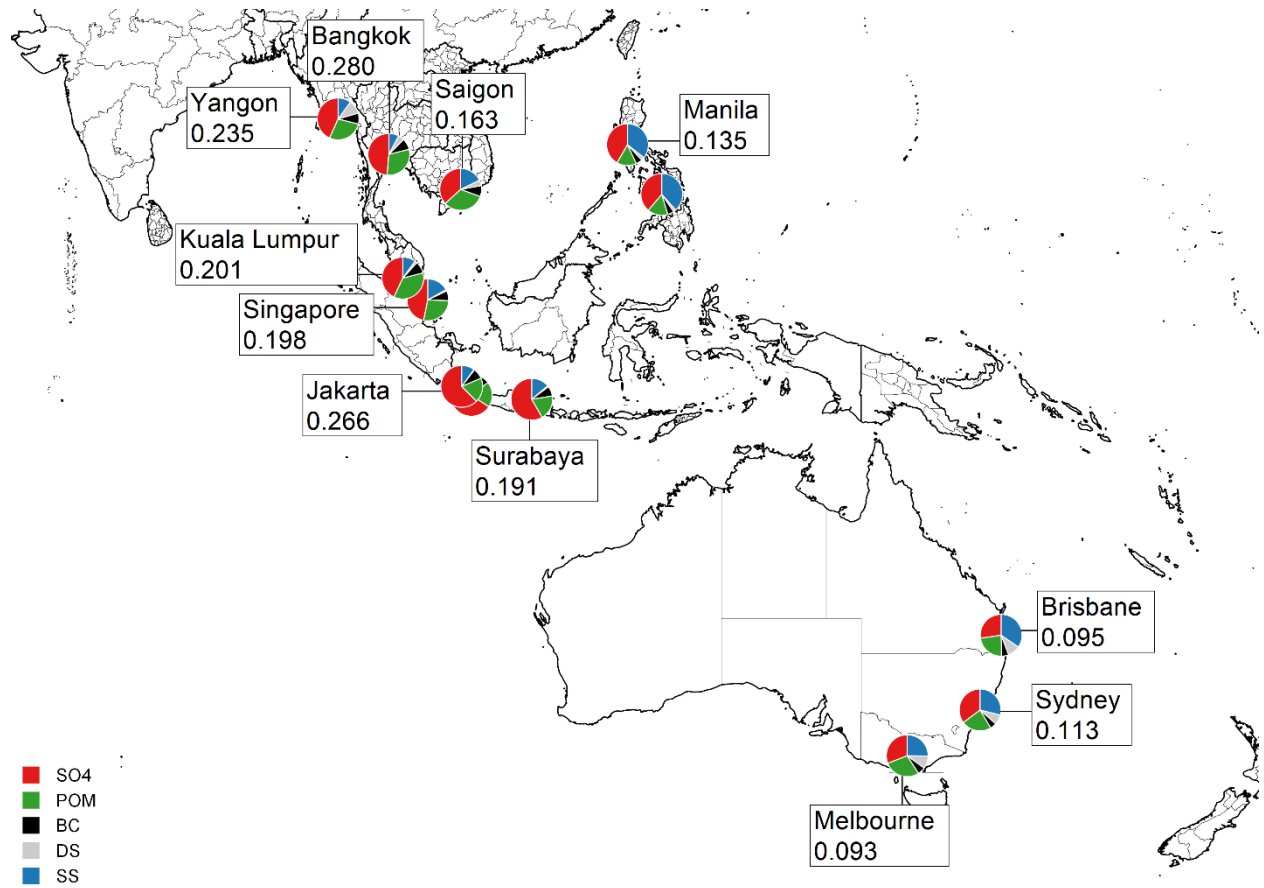


Figure 12

- Over 0.004/yr increase
- 0 to 0.004/yr increase
- Insignificant increase
- Insignificant decrease
- 0 to 0.004/yr decrease
- Over 0.004/yr decrease

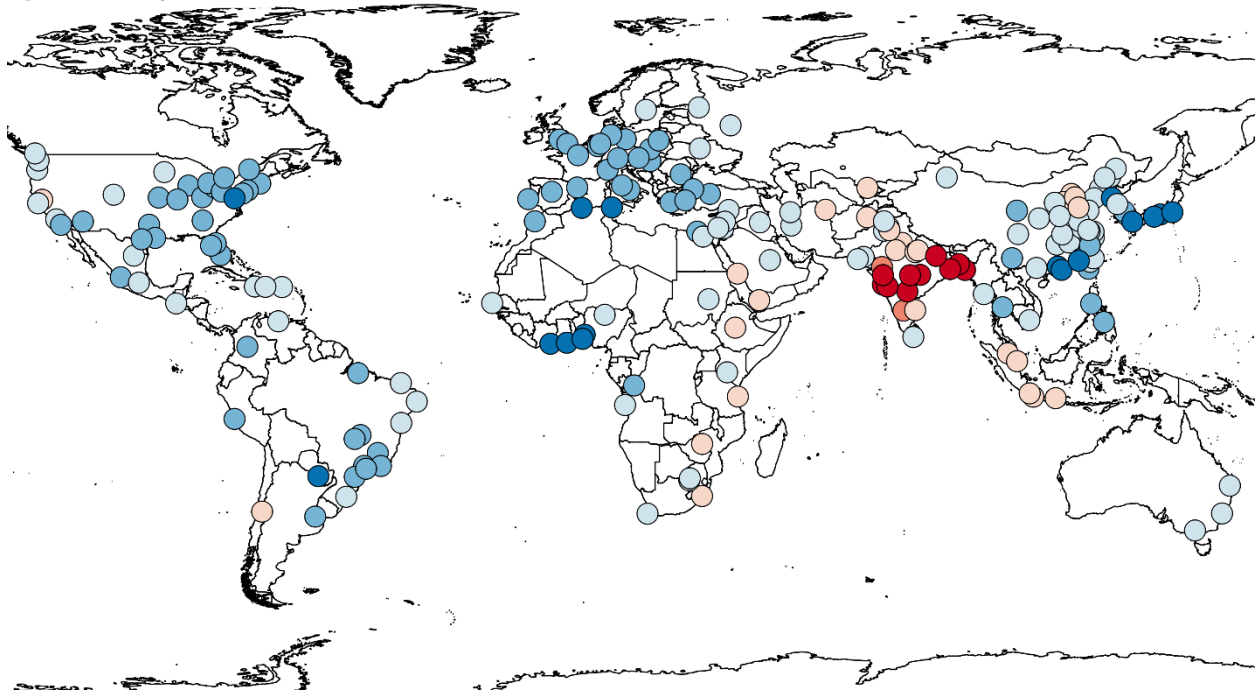


Figure 13

- Over 0.003/yr increase
- 0 to 0.003/yr increase
- Insignificant increase
- Insignificant decrease
- 0 to 0.003/yr decrease
- Over 0.003/yr decrease

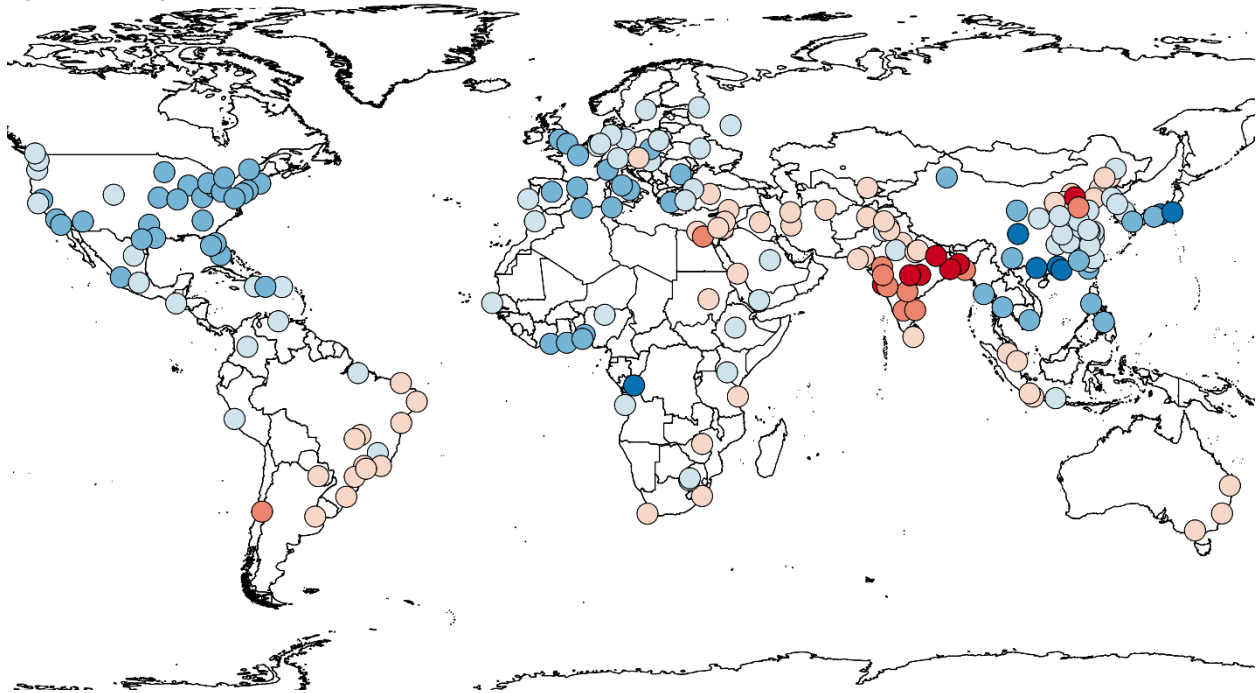




Figure 16

- Over 0.003/yr increase
- 0 to 0.003/yr increase
- Insignificant increase
- Insignificant decrease
- 0 to 0.003/yr decrease
- Over 0.003/yr decrease

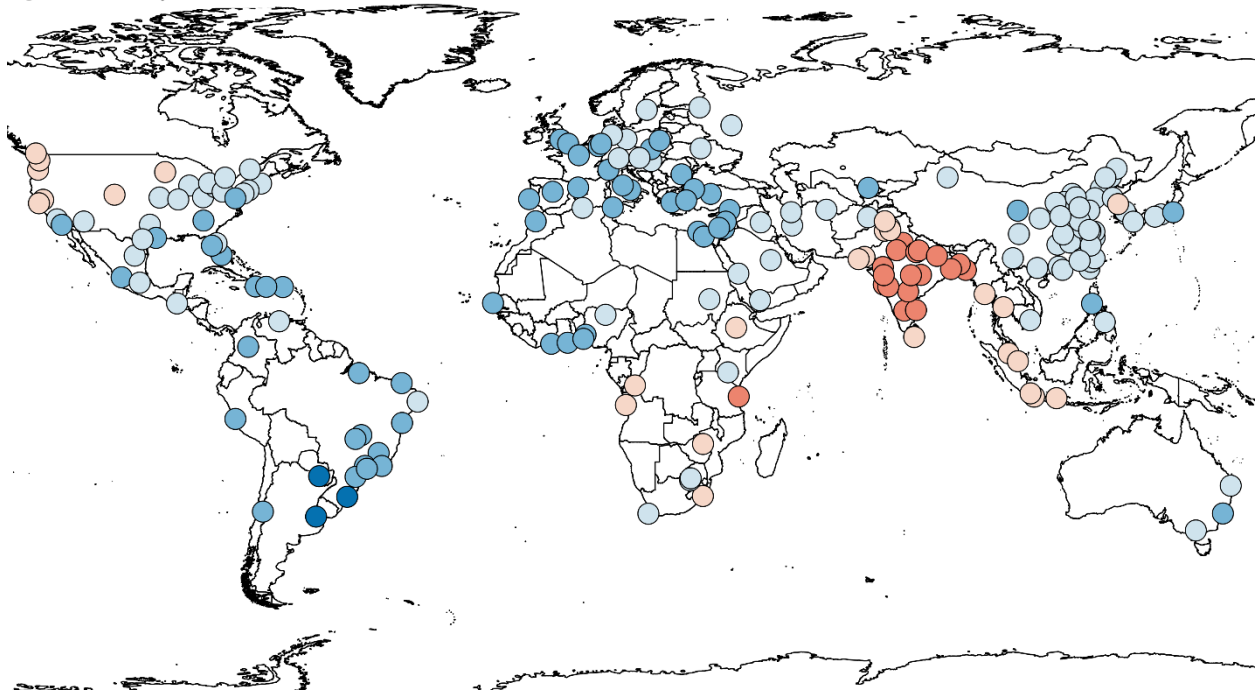


Figure 17

- Over 0.0005/yr increase
- 0 to 0.0005/yr increase
- Insignificant increase
- Insignificant decrease
- 0 to 0.0005/yr increase
- Over 0.0005/yr increase

